Design, synthesis, and evaluation of 5-methyl-4-phenoxy-5*H*-pyrrolo-[3,2-*d*]pyrimidine derivatives: Novel VEGFR2 kinase inhibitors binding to inactive kinase conformation

Yuya Oguro [a,*], Naoki Miyamoto [a], Kengo Okada [b], Terufumi Takagi [b], Hidehisa Iwata [b], Yoshiko Awazu [a], Hiroshi Miki [b], Akira Hori [a], Keiji Kamiyama [a], Shinichi Imamura [a]

[a] *Pharmaceutical Research Division, Takeda Pharmaceutical Co., Ltd, 10, Wadai, Tsukuba, Ibaraki 300-4293, Japan*
[b] *Pharmaceutical Research Division, Takeda Pharmaceutical Co., Ltd, 2-17-85, Jusohonmachi, Yodogawa-ku, Osaka 532-8686, Japan*

ABSTRACT

We synthesized a series of pyrrolo[3,2-*d*]pyrimidine derivatives and evaluated their application as type-II inhibitors of vascular endothelial growth factor receptor 2 (VEGFR2) kinase. Incorporation of a diphenyl-urea moiety at the C4-position of the pyrrolo[3,2-*d*]pyrimidine core via an oxygen linker resulted in compounds that were potent inhibitors of VEGFR2 kinase. Of these derivatives, compound **20d** showed the strongest inhibition of VEGF-stimulated proliferation of human umbilical vein endothelial cells (HUVEC). The co-crystal structure of **20d** and VEGFR2 revealed that **20d** binds to the inactive form of VEGFR2. Further studies indicated that **20d** inhibited VEGFR2 kinase with slow dissociation kinetics and also inhibited PDGFR and Tie-2 kinases. Oral administration of the hydrochloride salt of **20d** at 3 mg/kg/day showed potent inhibition of tumor growth in a DU145 human prostate cancer cell xenograft nude mouse model.

© 2010 Elsevier Ltd. All rights reserved.

1. Introduction

Angiogenesis, the formation of new capillary blood vessels from preexisting vasculature, is the process by which solid tumors are supplied with oxygen and nutrients.[1] Angiogenesis is increased in various types of cancers, and high microvessel density in the tumor correlates with poor prognosis in patients.[2,3] Therefore, the inhibition of tumor angiogenesis is considered to be a promising approach for the treatment of many human malignancies.[4]

The vascular endothelial growth factor (VEGF) family is a large family of angiogenic and lymphangiogenic growth factors, and VEGF plays an important role in tumor angiogenesis.[5] In solid tumors, VEGF expression is upregulated by cancer-related changes, such as proto-oncogene activation,[6] loss of tumor suppressor function,[7,8] growth factor stimuli,[9] and hypoxic status.[10,11] Angiogenesis is triggered by the binding of VEGF to vascular endothelial growth factor receptor (VEGFR); the different subtypes of VEGFR include VEGFR1 (also known as Flt1), VEGFR2 (also known as KDR), and VEGFR3 (also known as Flt4).[5] Binding of VEGF to VEGFR induces conformational changes in VEGFR followed by receptor dimerization, autophosphorylation of tyrosine residues in the intracellular kinase domain and exerts potent mitogenic and chemotactic effects on endothelial cells.[12] VEGF overexpression correlates with poor prognosis and clinical staging in the majority of solid tumor patients.[13–15] VEGF/VEGFR signaling is, therefore, regarded as an attractive therapeutic target for inhibition of tumor angiogenesis. Bevacizumab, a recombinant humanized monoclonal antibody against VEGF, has been approved as first-line therapy for various conditions such as metastatic colorectal cancer.[16–18]

The majority of known kinase inhibitors such as gefitinib are classified as type-I kinase inhibitors, which bind in and around the region occupied by the adenine ring of ATP.[19] On the other hand, type-II kinase inhibitors (e.g., imatinib) induce the DFG-out conformation of the activation loop, enabling them to occupy the adenine binding site and an adjacent hydrophobic pocket created by this rearrangement.[20] The X-ray co-crystal structures of kinase-bound type-II kinase inhibitors also generally reveal two conserved hydrogen-bond interactions between the ligand and protein: one with the side chain of a conserved glutamic acid in the αC-helix (Glu885 in VEGFR2), and the other with the backbone amide of aspartic acid in the DFG motif (Asp1046 in VEGFR2). Type-II kinase inhibitors have several advantages over type-I kinase inhibitors, including improved kinase selectivity and slower off-rates.[21,22] Therefore, we focused on the identification of novel type-II VEGFR kinase inhibitors. Studies to identify novel kinase inhibitors showed that the pyrrolo[3,2-*d*]pyrimidine scaffold could serve as a novel kinase hinge binding template.[23] This finding

* Corresponding author. Tel.: +81 29 864 6384; fax: +81 29 864 6308.
  E-mail address: Ooguro_Yuuya@takeda.co.jp (Y. Oguro).

encouraged us to generate novel type-II kinase inhibitors by incorporating a substituted benzene ring at the C4-position of the pyrrolo[3,2-*d*]pyrimidine core via an appropriate linker (X) (Fig. 1). To rationalize the designed compound as a good starting point for type-II inhibitors, the binding model of VEGFR2 with the pyrrolo[3,2-*d*]pyrimidine derivative (A) (X = O, R′ = H, Y-R = H in Fig. 1) was generated. The binding model suggested the N1-nitrogen of the pyrrolo[3,2-*d*]pyrimidine interacts with the main chain NH group of Cys919 in the hinge region and the phenoxy group extended toward the back hydrophobic pocket. Thus, we designed the compounds possessing a hydrogen bond donor–acceptor pair (Y) and a lipophilic group (R) on the benzene ring, aiming interaction with Glu885, Asp1046, and the hydrophobic pocket. In this paper, we report the synthesis, structure–activity relationships (SAR), and characterization of these new inhibitors.

2. Chemistry

A general synthesis of 4-phenoxy-pyrrolo[3,2-*d*]pyrimidine derivatives possessing urea, amide, thiourea, and benzimidazole functionalities is shown in Schemes 1 and 2. Synthesis was initiated by treating pyrrolo[3,2-*d*]pyrimidine 1[24,25] with methyl methanesulfonate to afford 2, which was coupled with 3- or 4-aminophenol in the presence of potassium carbonate to provide aniline 3 or 6, respectively. Aniline 3 was converted to the corresponding urea 4 or amide 5 using phenyl isocyanate or benzoyl chloride, respectively. Aniline 6 was also converted to ureas 7a–j, amides 8 and 9, thiourea 10, and benzimidazole 11. The ureas 7a–j were formed by reaction of 6 and the corresponding amines with *N,N*-carbonyldiimidazole (CDI), or by reaction with the corresponding isocyanates. The amides 8 and 9, and thiourea 10 were obtained by treatment of 6 with benzoyl chloride, phenylacetyl chloride, or phenyl isothiocyanate, respectively. In addition, the benzimidazole 11 was synthesized via reaction of 6 with 2-chlorobenzimidazole.

Benzoic acids 12a,b and ester 14, which were prepared by coupling 2 with the corresponding phenols, were used for the synthesis of amides 13a,b and 16 (Scheme 2). Condensation of 12a,b with aniline using 1-ethyl-3-(3-dimethylaminopropyl) carbodiimide hydrochloride (EDCI·HCl) and 1-hydroxybenzotriazole (HOBt) provided 13a,b, respectively. Similarly, the phenylacetic acid derivative 15, which was obtained by hydrolysis of 14, was converted to amide 16.

Modification of the linker atoms between the pyrrolo[3,2-*d*]pyrimidine core and the central phenyl ring was accomplished as shown in Scheme 3. Thioether 17a was readily prepared by

coupling of 2 and 4-aminothiophenol in a manner similar to the synthesis of ether 6. In contrast, 17b,c, which have nitrogen linkers, were not obtained under the same conditions as the synthesis of 17a. Consequently, coupling of 2 with 4-nitroaniline under acidic conditions followed by hydrogenation successfully provided 17b. In the same manner, coupling of 2 with *N*-methyl-4-nitroaniline using sodium hydride and subsequent hydrogenation gave 17c. Treatment of anilines 17a–c with the appropriate phenyl isocyanates provided the corresponding ureas 18a–c.

Urea derivatives possessing various substituents on the central phenyl ring (20a–d) were prepared as shown in Scheme 4. While direct coupling of 2 with the corresponding aminophenols in the presence of K₂CO₃ provided the 2-chloro-, 3-chloro-, and 2-methoxyanilines 19a–c in good yield, synthesis of the 2-fluoroaniline derivative 19d was unsuccessful under these basic conditions due to the self-coupling of 3-fluoro-4-aminophenol. Thus, 19d was prepared by coupling of 2 with 3-fluoro-4-nitrophenol without base followed by reduction with zinc. The anilines 19a–d were converted to the corresponding ureas 20a–d by treatment with 3-(trifluoromethyl)phenyl isocyanate.

The synthesis of the pyrrolo[3,2,1-*de*]pteridine derivative 23 is presented in Scheme 5. Pyrrolo[3,2-*d*]pyrimidine 1 was alkylated with 2-bromo-1-chloroethane to give 21, which was converted to 22 by coupling with aniline 25. Compound 22 was then cyclized in the presence of K₂CO₃ to provide pyrrolo[3,2,1-*de*]pteridine 23. Aniline 25 was synthesized by reaction of the 4-nitroaniline 24 with 3-(trifluoromethyl)phenyl isocyanate and subsequent hydrogenation using Pd/C.

3. Results and discussion

The pyrrolo[3,2-*d*]pyrimidine derivatives depicted in Tables 1–4 were evaluated for their inhibitory activity against human VEGFR2 kinase by a non-RI assay using the amplified luminescent proximity homogeneous assay (AlphaScreen®) system. AlphaScreen® is based on the transfer of energy from donor to acceptor microbeads brought together by a biomolecular interaction.[26] In this system, an anti-phosphotyrosine antibody is immobilized with acceptor beads, and the biotinylated poly-GluTyr (4:1) is conjugated with streptavidin donor beads. The amount of phosphorylated substrate is measured as a signal of AlphaScreen®. Subsequently, a cell proliferation assay was performed to investigate the potent VEGFR2 kinase inhibitors among these compounds for their ability to inhibit VEGF-stimulated proliferation of human umbilical vein endothelial cells (HUVEC).
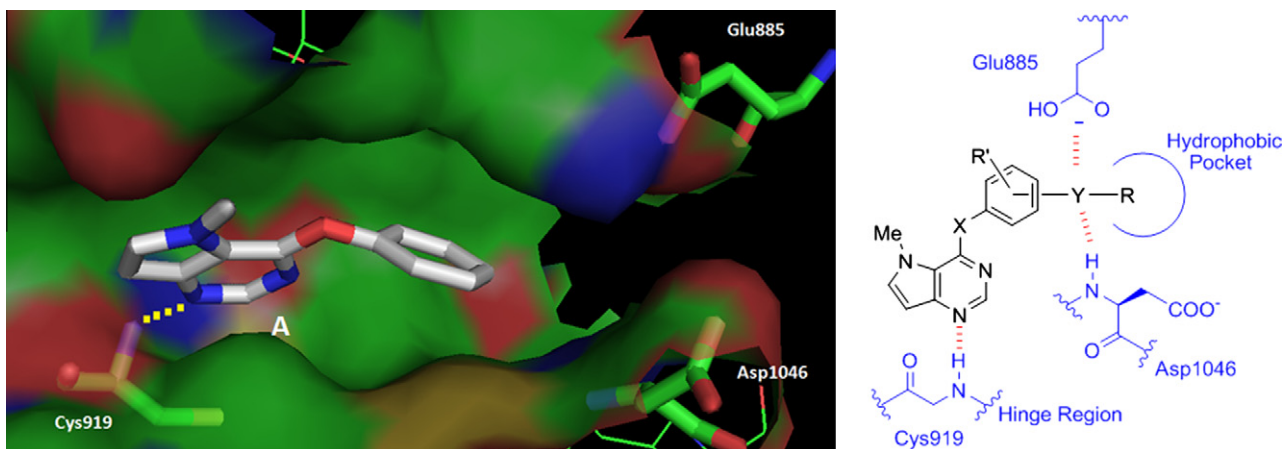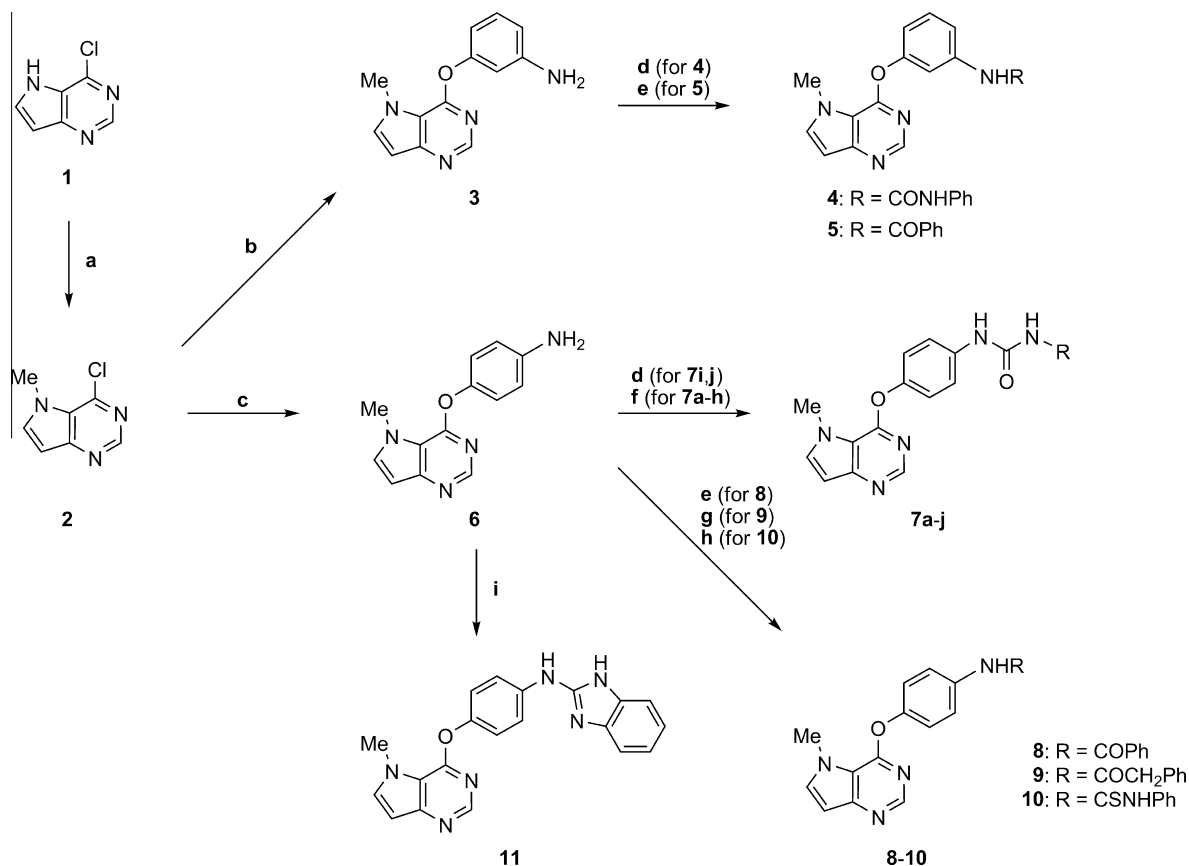

Figure 1. Design of pyrrolo[3,2-*d*]pyrimidine derivatives. Molecular modeling study of the pyrrolo[3,2-*d*]pyrimidine derivative A was carried out using the program GOLD and the X-ray structure of VEGFR2 (PDB code: IVR2).
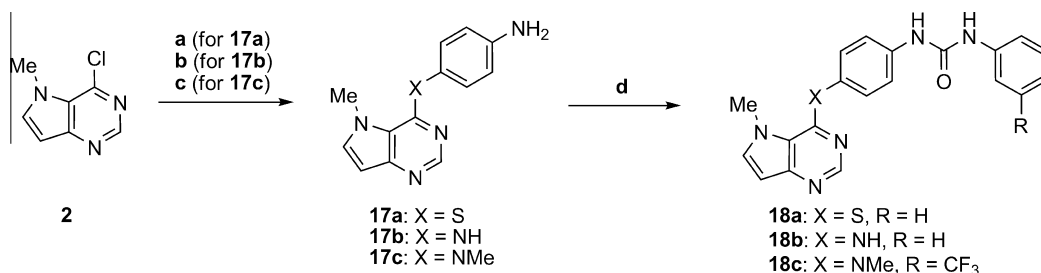
Scheme 1. Reagents and conditions: (a) MsOMe, Cs_2CO_3, DMF, rt; (b) 3-aminophenol, K_2CO_3, NMP, 110 °C; (c) 4-aminophenol, K_2CO_3, NMP, 110 °C; (d) phenyl isocyanates, Et_3N, THF, rt; (e) PhCOCl, Et_3N, THF, rt; (f) amines, CDI, DMF, rt; (g) $PhCH_2COCl$, Et_3N, THF, rt; (h) PhNCS, Et_3N, THF, rt; (i) 2-chlorobenzimidazole, NMP, 120 °C.
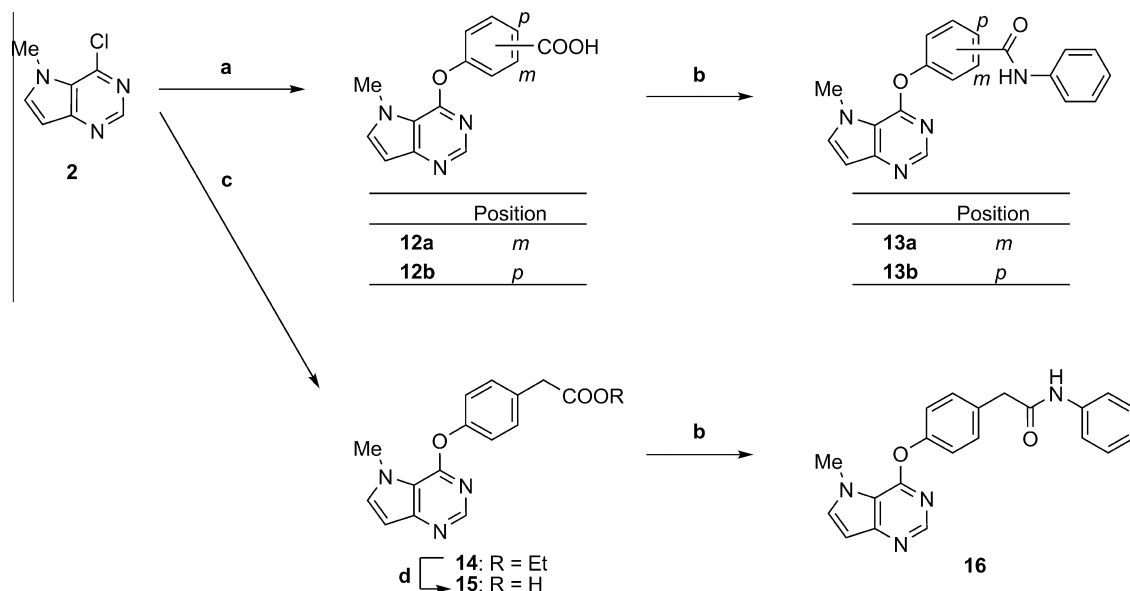

Scheme 2. Reagents and conditions: (a) 3- or 4-Hydroxybenzoic acid, Cs_2CO_3, DMSO, 100 °C; (b) aniline, EDCI·HCl, HOBt, DMF, rt; (c) ethyl 4-hydroxyphenylacetate, K_2CO_3, NMP, 110 °C; (d) NaOH, H_2O, MeOH, rt.

We introduced appropriate substituents into the phenoxy group at C4-position of pyrrolo[3,2-d]pyrimidine considered the interactions between Glu885/Asp1046 and the hydrophobic pocket of VEGFR2, which is seen in many type-II kinase inhibitors (Table 1). The initial compounds evaluated from this series were the

3′-phenylurea and 3′-phenylamide derivatives **4, 5**, and **13a**, which showed inhibitory activity toward VEGFR2 kinase with IC_{50} values of around 1000 nM. The moderate potencies shown by **4, 5**, and **13a** suggested that they might serve as good starting points for the development of potent type-II VEGFR2 kinase inhibitors.

Scheme 3. Reagents and conditions: (a) 4-Aminothiophenol, K_2CO_3, NMP, 110 °C; (b) (1) 4-nitroaniline, 2-propanol, 4 M HCl/AcOEt, 80 °C; (2) H_2, Pd/C, MeOH, rt; (c) N-methyl-4-nitroaniline, NaH, DMF, 0 °C to rt; (2) H_2, Pd/C, MeOH, rt; (d) phenyl isocyanates, Et$_3$N, THF, rt.
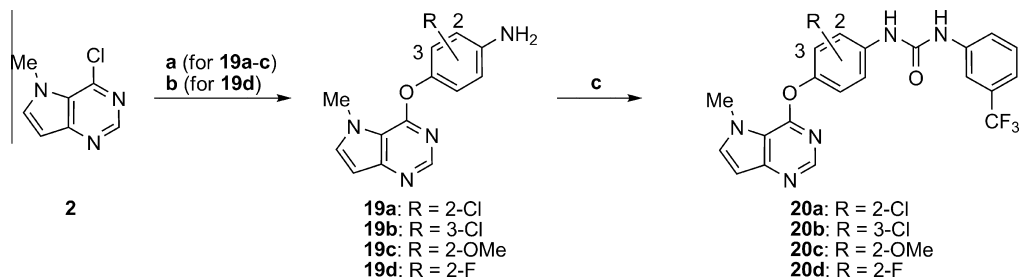

Scheme 4. Reagents and conditions: (a) Aminophenols, K_2CO_3, NMP, 110 °C; (b) (1) 3-fluoro-4-nitrophenol, o-xylene, 100 °C; (2) Zn, NH$_4$Cl, MeOH, reflux; (c) 3-(trifluoromethyl)phenyl isocyanate, Et$_3$N, THF, rt.
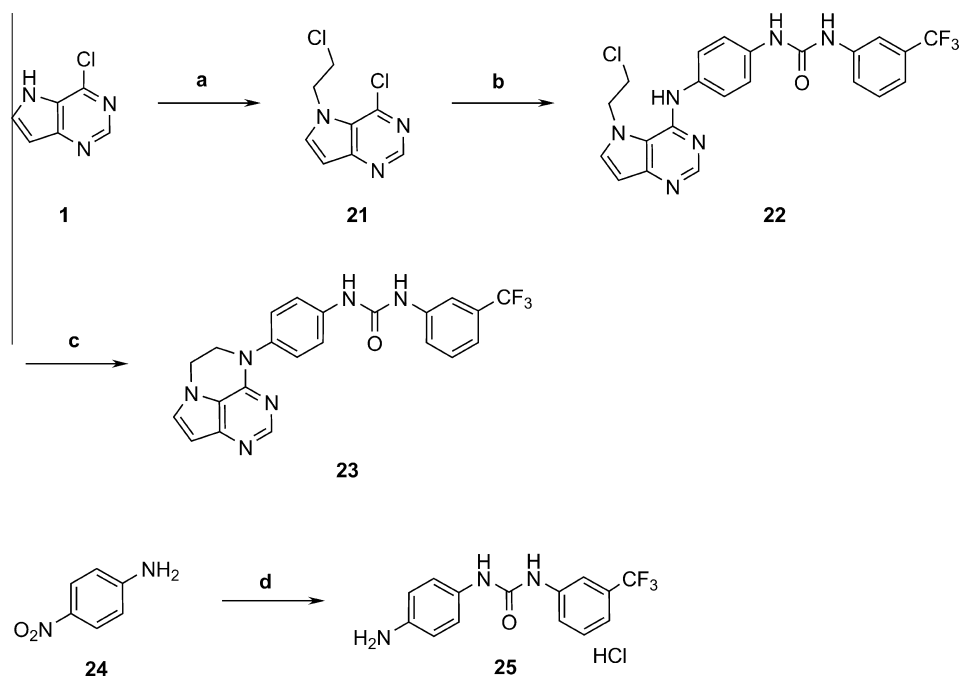

Scheme 5. Reagents and conditions: (a) 2-Bromo-1-chloroethane, Cs$_2$CO$_3$, DMF, rt; (b) **25**, 2-propanol, 80 °C; (c) K$_2$CO$_3$, DMF, 80 °C; (d) (1) 3-(trifluoromethyl)phenyl isocyanate, Et$_3$N, THF, rt; (2) H$_2$, Pd/C, MeOH, rt; (3) 4 M HCl/AcOEt, AcOEt, rt.

Further investigation revealed that moving the phenylureido group of **4** from the 3′-position to the 4′-position (**7a**) significantly increased potency (**7a**: IC$_{50}$ = 33 nM), while the potency did not increased by similar modification of 3′-phenylamides **5** and **13a** to the corresponding 4′-phenylamides **8** and **13b** (**8**: IC$_{50}$ = 9400 nM, **13b**: IC$_{50}$ >10,000 nM). The importance of the urea linker was also shown by the significant loss of potency observed for the amides **9** and **16** and for the thiourea **10**. The amide derivatives **9** and **16**, which have a carbon in place of the ureido nitrogen of the urea

7a, were >300- and 100-fold less active than **7a**, respectively. Thiourea **10** also exhibited an approximate 200-fold loss of potency. These results indicated that all of the NH groups and the oxygen in the urea of **7a** might be involved in hydrogen bonding with VEGFR2. The benzimidazole derivative **11** was designed to examine the potential of using the benzimidazole moiety as an isosteric replacement for the biphenylurea side chain. However, **11** was found to be less potent than **7a** (**11**: IC$_{50}$ = 4200 nM), revealing that it was less suited for hydrogen bonding with VEGFR2 than **7a**.

Table 1
Inhibitory activity of pyrrolo[3,2-d]pyrimidine derivatives against vascular endothelial growth factor receptor 2 kinase[a]
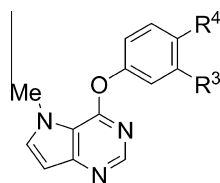
Compd	R³	R⁴	VEGFR2 IC$_{50}$ (nM)
4	NHCONHPh	H	1800 (1600–2200)
5	NHCOPh	H	940 (770–1100)
13a	CONHPh	H	870 (740–1000)
7a	H	NHCONHPh	33 (27–40)
8	H	NHCOPh	9400 (7000–13,000)
13b	H	CONHPh	>10,000
9	H	NHCOCH$_2$Ph	>10,000
16	H	CH$_2$CONHPh	3300 (2400–4500)
10	H	NHCSNHPh	6700 (5200–8800))
11	H		4200 (3200–5600)

[a] Numbers in parentheses represent 95% confidence interval.

Table 2
Effect of urea substituents on vascular endothelial growth factor receptor 2 kinase and cellular growth inhibition[a]
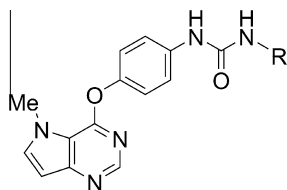
Compd	R	VEGFR2 IC$_{50}$ (nM)	HUVEC[b] IC$_{50}$ (nM)
7a	Ph	33 (27–40)	810 (630–1000)
7b	Me	6300 (4800–8400)	24,000 (21,000–27,000)
7c	Pr	3900 (3300–4600)	24,000 (21,000–27,000)
7d	2-ClPh	340 (280–400)	2700 (2300–3200)
7e	3-ClPh	4.1 (3.4–5.0)	110 (84–130)
7f	4-ClPh	32 (26–40)	1100 (940–1300)
7g	3-CF$_3$Ph	5.3 (4.4–6.3)	22 (16–30)
7h	3-BrPh	4.4 (3.9–5.1)	44 (31–63)
7i	3-FPh	19 (16–22)	290 (230–370)
7j	3-MePh	2.7 (2.3–3.1)	62 (38–110)

[a] Numbers in parentheses represent 95% confidence interval.
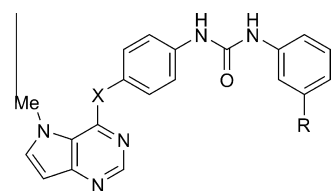[b] Growth inhibition of human umbilical vein endothelial cells (HUVEC).

Thus, we concluded that a 4′-urea substituent on the 4-phenoxy-5H-pyrrolo[3,2-d]pyrimidine scaffold was optimal for the inhibition of VEGFR2 kinase, and then, we examined the urea substituents. The results in Table 2 show that phenyl groups seemed to be more preferred as urea substituents than smaller aliphatic groups. Replacement of phenyl (**7a**) with methyl (**7b**) or propyl (**7c**) brought >100-fold loss of inhibitory activity against VEGFR2 kinase, indicating that the small lipophilic substituents were insufficient to occupy the hydrophobic pocket. Systematic investigation of substituents placed at the *ortho*-, *meta*-, and *para*-positions of the urea phenyl ring revealed that a *meta*-substituted phenyl was optimal for inhibitory activity against VEGFR2 kinase (**7e** vs **7d**,**f**). In addition to the increased enzymatic activity, **7e** also displayed moderate cellular potency (HUVEC IC$_{50}$ = 110 nM) in the VEGF-driven HUVEC proliferation assay. Optimization of substituents at the *meta*-position revealed that very potent inhibitory activity against VEGFR2 kinase
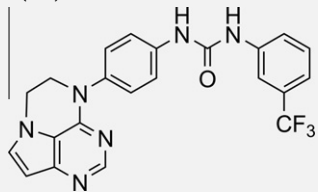
was achieved by the introduction of a trifluoromethyl group (**7g**: IC$_{50}$ = 5.3 nM), bromine atom (**7h**: IC$_{50}$ = 4.4 nM), or methyl group (**7j**: IC$_{50}$ = 2.7 nM) although the smaller fluorine atom (**7i**: IC$_{50}$ = 19 nM) showed slightly decreased activity. It is noteworthy that the *meta*-CF$_3$ derivative (**7g**) yielded cellular potency (HUVEC IC$_{50}$ = 22 nM) quite close to the inhibitory activity against VEGFR2 kinase.
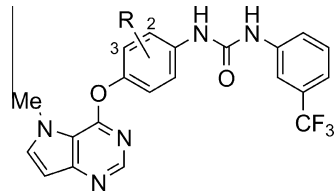
Optimization of the linker atom between the pyrrolo[3,2-d]-pyrimidine core and the central phenyl ring revealed that an oxygen linker is preferred to sulfur or nitrogen (Table 3). In fact, the sulfur linker derivative (**18a**: IC$_{50}$ = 110 nM) was threefold less active than the oxygen linker derivative (**7a**), while the amino linker derivative (**18b**: IC$_{50}$ = 1400 nM) exhibited 40-fold loss of potency. Based on their decreased enzymatic activity, **18a**,**b** showed the declined HUVEC inhibitory activity. On the other hand, a significant reduction in activity was observed with an *N*-methylamino linker (**18c**: IC$_{50}$ >10000 nM), suggesting that steric hindrance between the methyl group on the linker nitrogen and the methyl group at the N5-position of the pyrrolo[3,2-d]pyrimidine core causes destabilization of the active conformation. The recovery of activity by cyclization between the nitrogen linker and the N-5 nitrogen (**23**: IC$_{50}$ = 7.1 nM) supports this hypothesis.

The effects of substituents on the central phenyl group were also investigated (Table 4). Introduction of a chlorine atom into the central phenyl ring of **7g** revealed that substitution at the 2-position was more promising than the 3-position. The 2-chloro compound **20a** was twofold more potent in cellular assay compared to **7g**, whereas the 3-chloro compound **20b** exhibited a decreased potency in both kinase and cellular assays. As a result of further investigations, the 2-fluorine substituted compound **20d** was found to show the strongest HUVEC inhibitory activity with an IC$_{50}$ value of 4.4 nM. On the other hand, replacement of the fluorine (**20d**) with a methoxy group (**20c**) resulted in decreased enzyme and cell activity. There are three possible explanation for decreased potency observed for **20c**: the methoxy group may relatively too big to occupy the binding pocket around the central phenyl ring, the steric hindrance between the methoxy group and the ureido moiety of **20c** may destabilize the active conformation, the lowered acidity of ureido moiety may cause the decreased interaction between the ureido moiety and amino acid residues in the protein. Pharmacokinetic parameters for the compounds were obtained by cassette dosing in mice. After oral administration (10 mg/kg), compound **20d** showed an area under the plasma concentration-time curve (AUC$_{0-8\,h}$) equal to 10.9 µg h/mL. Furthermore, the plasma concentration of **20d** at 8 h after administration (C$_{8\,h}$) was 410-fold higher than its IC$_{50}$ value in HUVEC assay (C$_{8\,h}$ = 0.803 µg/mL = 1.8 µM). On the basis of these results, we selected **20d** for further evaluation.

In order to confirm the binding mode of **20d**, the co-crystal structure of the complex between **20d** and VEGFR2 was obtained (Fig. 2). The kinase adopts an inactive conformation (DFG-out) so that the urea portion occupies the back hydrophobic pocket with additional hydrogen-bonding interactions. The N1-nitrogen of the pyrrolo[3,2-d]pyrimidine core interacts with the main chain NH group of Cys919 in the hinge region. The urea moiety binds to the protein through two hydrogen-bonding interactions: both urea NH groups interact with Glu885, and the carbonyl interacts with Asp1046. Compounds missing one of the NH groups (**9** or **16**) or the carbonyl oxygen (**10**) bind more weakly to the protein, suggesting that all of these hydrogen bonds contribute significantly to the binding affinity. The external 3-(trifluoromethyl)phenyl moiety occupies the hydrophobic pocket created by the conformational rearrangement of Phe1047 (DFG-out). We can rationalize that the significant loss of activity caused by replacement of phenyl (**7a**: VEGFR2 IC$_{50}$ = 33 nM) with methyl (**7b**: VEGFR2 IC$_{50}$ = 6300 nM) is probably due to insufficient occupation of this extended hydrophobic pocket.

Table 3
Effect of linker atoms on vascular endothelial growth factor receptor 2 kinase and cellular growth inhibition[a]

Compd	X	R	VEGFR2 IC$_{50}$ (nM)	HUVEC[b] IC$_{50}$ (nM)
7a	O	H	33 (27–40)	810 (630–1000)
7g	O	CF$_3$	5.3 (4.4–6.3)	22 (16–30)
18a	S	H	110 (65–170)	35% inhibition at 1 μM
18b	NH	H	1400 (1200–1600)	<10% inhibition at 1 μM
18c	N(Me)	CF$_3$	>10,000	<10% inhibition at 1 μM
23			7.1 (6.3–8.1)	230 (170–310)

[a] Numbers in parentheses represent 95% confidence interval.
[b] Growth inhibition of human umbilical vein endothelial cells (HUVEC).

Table 4
Effects of central phenyl ring substituents on in vitro and pharmacokinetic properties[a]

Compd	R	VEGFR2 IC$_{50}$ (nM)	HUVEC[b] IC$_{50}$ (nM)	Mice PK[c]	
				AUC$_{0-8\ h}$[d] (μg h/mL)	C$_{8h}$[e] (μg/mL)
7g	H	5.3 (4.4–6.3)	22 (16–30)	11.7	0.570
20a	2-Cl	3.7 (3.4–4.1)	13 (8.6–20)	10.5	0.843
20b	3-Cl	30 (25–36)	39 (25–60)	9.10	0.584
20c	2-OMe	14 (11–17)	87 (74–103)	14.7	0.572
20d	2-F	6.2 (4.7–8.3)	4.4 (3.0–6.4)	10.9	0.803

[a] Numbers in parentheses represent 95% confidence interval.
[b] Growth inhibition of human umbilical vein endothelial cells (HUVEC).
[c] Compounds were orally administered at a dose of 10 mg/kg by cassette dosing.
[d] Area under the plasma concentration-time curve (μg h/mL).
[e] Plasma concentration at 8 h after administration.

To characterize the mode of inhibitory activity of **20d**, we measured the recovery of enzymatic activity after a large dilution of the VEGFR2-**20d** complex (Fig. 3).[27,28] After the preformed complex of **20d** and VEGFR2 was diluted to one tenth of IC$_{50}$ with buffer including 1 mM of ATP, the recovery of kinase activity was much slower than control (no inhibitor). The progress curve for the control reaction (no inhibitor) was essentially linear for 2000 second after dilution. In contrast, the activity of VEGFR2 kinase pre-incubated with **20d** was very low at that time, indicating a unique mode of **20d** to inhibit VEGFR2 kinase with very slow dissociation kinetics. This result suggests DFG-out conformation of VEGFR2 induced by **20d** seems very stable. Slow dissociation kinetics and lack of biochemical evidence for the formation of an irreversible covalent bond is called pseudo-irreversible inhibition.[29,30] Thus, **20d** is pseudo-irreversible inhibitor and may show prolonged action against VEGFR2 kinase in both in vitro and in vivo settings.

Compound **20d** was tested for selectivity with respect to other kinases (Table 5). Compound **20d** inhibited VEGFR2, tyrosine kinase with Ig and EGF homology domains-2 (Tie-2), and platelet-derived growth factor receptors β (PDGFRβ) kinases with IC$_{50}$ values of 6.2, 20, and 96 nM, respectively. These kinases are close to each other in the kinome tree.[31] In addition to VEGF/VEGFR, angiopoietin/Tie-2 and platelet-derived growth factors (PDGF)/PDGFR signals play important roles in angiogenesis. Tyrosine phosphorylation of Tie-2 by its ligand angiopoietin-1 (Ang-1) is involved in more mature angiogenic processes, such as vessel branching, sprouting, remodeling, maturation, and stability.[32] Activation of PDGF/PDGFR signal also induce proliferation and migration of pericytes, which leads to the formation of thicker and more stable blood vessels.[33,34] Therefore, these additional kinase inhibitory activities of **20d** may be beneficial for its antiangiogenic activity. On the other hand, IC$_{50}$ values against other protein kinases such as fibroblast growth factor receptor 1 (FGFR1), human epidermal growth factor receptor 2 (HER2),
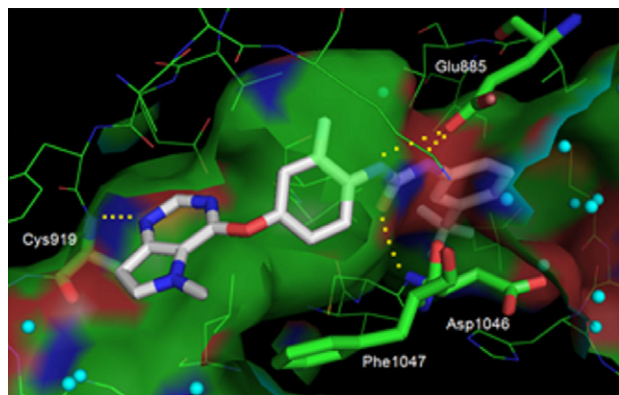
Figure 2. X-ray co-crystal structure of **20d** in complex with VEGFR2.
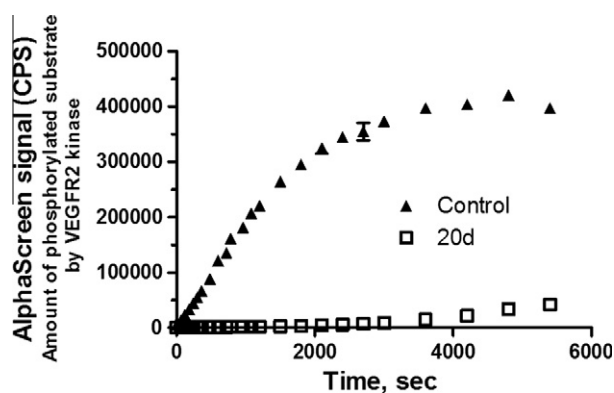

Figure 3. Dilution assay of VEGFR2-**20d** complex. Phosphorylation of peptide substrate as a function of time is shown. The reaction was initiated by diluting a preformed enzyme–inhibitor complex to one tenth of IC_{50} with reaction buffer containing 1 mM ATP and 0.1 µg/mL biotinylated poly-GluTyr (4:1). The recovery of activity was measured using the AlphaScreen® system.

Table 5
Kinase inhibition profile of **20d**[a,b]

Kinase	IC_{50} (nM)	Kinase	IC_{50} (nM)
VEGFR2	6.2 (4.7–8.3)	IGF-1-R	>10,000
VEGFR1	15 (14–17)	c-kit	170 (120–240)
PDGFRα	35 (27–43)	Src	>10,000
PDGFRβ	96 (76–120)	FAK	2600 (2000–3400)
FGFR1	>10,000	B-raf	900 (660–1200)
Tie-2	20 (17–23)	ERK1	>10,000
HER2	>10,000	PKCθ	>10,000
EGFR	>10,000	GSK3β	>10,000
IR	>10,000	AurolaA	1050 (660–1700)

[a] Abbreviations of kinases are described in Section 5.
[b] Numbers in parentheses represent 95% confidence interval.

epidermal growth factor receptor (EGFR), insulin receptor (IR), and protein kinase C θ (PKCθ) were over 10,000 nM.

Finally, we evaluated the antitumor effects of the hydrochloride salt of **20d** in a xenograft nude mouse model with the human DU145 prostate cancer cell line which is known to produce VEGF (Fig. 4).[35] Consistent with its potent in vitro activities and good oral exposure levels, oral administration of the hydrochloride salt of **20d** twice daily at 1.5, 3, 6, and 12 mg/kg for 21 days led to significant antitumor effects with T/C (treatment over control) values of 38%, 15%, 1%, and −8%, respectively. Under these conditions, neither body weight loss nor obvious signs of toxicity were observed (data not shown). The slow dissociation kinetics and potent angio-
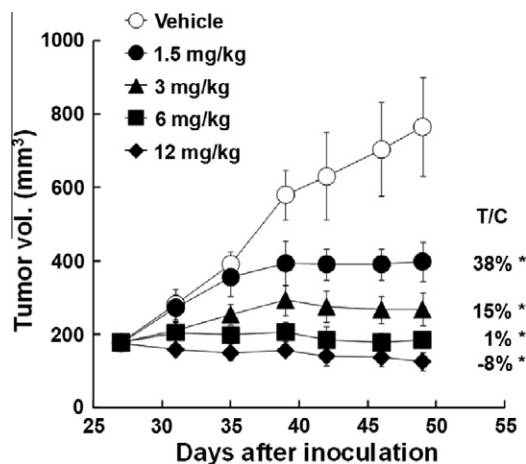

Figure 4. Efficacy of the hydrochloride of **20d** in DU145 tumor xenograft model. DU145 tumor-bearing mice were orally administered with the hydrochloride of **20d** (1.5, 3, 6, and 12 mg/kg) twice daily for 21 days. Data are shown as mean (standard deviation, SD) ($n = 5$). *: $p \leqslant 0.025$ versus vehicle control as determined by a one-tailed Williams' test. Antitumor effects expressed as T/C (growth of treated tumor/growth of control tumor) × 100.

genesis-related multikinase inhibitory activity of **20d** may contribute to its potent antitumor activity.

4. Conclusion

In order to generate novel type-II inhibitors of VEGFR kinase, we designed and synthesized a series of pyrrolo[3,2-d]pyrimidine derivatives. Incorporation of a diphenylurea moiety at the C4-position of the pyrrolo[3,2-d]pyrimidine core via an oxygen linker afforded potent VEGFR2 kinase inhibitors. Moreover, *meta*-substitution of the urea terminal benzene ring and substitution with a small lipophilic group at the 2-position of the central benzene ring enhanced HUVEC inhibitory activity. In particular, compound **20d** was extremely potent, with an IC_{50} value of 4.4 nM. A co-crystal structure between **20d** and VEGFR2 revealed that **20d** binds to the inactive conformation of VEGFR2, in which its diphenylurea moiety occupies the back hydrophobic pocket created by the conformational change of DFG motif (DFG-out). Results of further studies indicated that **20d** inhibited PDGFR and Tie-2 kinases in addition to VEGFR kinase and displayed slow dissociation kinetics. Oral treatment with the hydrochloride salt of **20d** showed potent antitumor effects in a DU145 mouse xenograft model. Thus, the slow dissociation kinetics and potent angiogenesis-related multikinase inhibitory activities of this compound class hold great promise as anticancer agents. Further modification using this urea series will be reported in due course.

5. Experimental

Melting points were determined on a BÜCHI Melting Point B-545, and were not corrected. Proton nuclear magnetic resonance (^{1}H NMR) spectra were recorded on Varian Mercury 300 (300 MHz) or Bruker DPX300 (300 MHz) instruments. Chemical shifts are reported as δ values (ppm) downfield from internal tetramethylsilane of the indicated organic solution. Peak multiplicities are expressed as follows: s, singlet; d, doublet; t, triplet; q, quartet; dd, doublet of doublet; ddd, doublet of doublet of doublets; dt, doublet of triplet; br s, broad singlet; m, multiplet. Coupling constants (*J* values) are given in hertz (Hz). Element analyses were carried out by Takeda Analytical Laboratories. Reaction progress was determined by thin layer chromatography (TLC) analysis on Silica Gel 60 F254 plate (Merck)

or NH TLC plates (Fuji Silysia Chemical Ltd). Chromatographic purification was carried on Silica Gel columns 60 (0.063–0.200 mm or 0.040–0.063 mm, Merck), basic silica gel (ChromatorexNH, 100–200 mesh, Fuji Silysia Chemical Ltd) or Purif-Pack (SI 60 lM or NH 60 lM, Fuji Silysia Chemical Ltd). Commercial reagents and solvents were used without additional purification. Abbreviations are used as follows: CDCl₃, deuterated chloroform; DMSO-d_6, dimethyl sulfoxide-d_6; AcOEt, ethyl acetate; DMF, N,N-dimethylformamide; MeOH, methanol; THF, tetrahydrofuran; EtOH, ethanol; DMSO, dimethyl sulfoxide; NMP, N-methylpyrrolidone.

5.1. 4-Chloro-5-methyl-5H-pyrrolo[3,2-d]pyrimidine (2)

A mixture of **1** (5.01 g, 32.5 mmol), methyl methanesulfonate (3.07 g, 34.2 mmol), cesium carbonate (21.2 g, 65.2 mmol), and DMF (50 mL) was stirred at room temperature for 15 h. The mixture was diluted with water and extracted with AcOEt. The extract was washed with brine, dried over anhydrous magnesium sulfate, and concentrated under reduced pressure to give **2** (4.36 g, 80%) as a pale yellow solid: ¹H NMR (DMSO-d_6) δ 4.09 (3H, s), 6.67–6.68 (1H, m), 7.95 (1H, d, J = 3.0 Hz), 8.57 (1H, s).

5.2. 3-[(5-Methyl-5H-pyrrolo[3,2-d]pyrimidin-4-yl)oxy]aniline (3)

A mixture of **2** (2.08 g, 9.83 mmol), 3-aminophenol (1.29 g, 11.8 mmol), potassium carbonate (3.26 g, 23.6 mmol), and NMP (15 mL) was stirred at 110 °C for 2 h. The mixture was diluted with water and extracted with AcOEt. The extract was washed with brine, dried over anhydrous magnesium sulfate, and concentrated under reduced pressure to give **3** (1.46 g, 62%) as a white solid: ¹H NMR (DMSO-d_6) δ 4.07 (3H, s), 5.28 (2H, br s), 6.34–6.50 (3H, m), 6.58 (1H, d, J = 3.2 Hz), 7.06 (1H, t, J = 7.8 Hz), 7.76 (1H, d, J = 3.2 Hz), 8.28 (1H, s).

5.3. 1-{3-[(5-Methyl-5H-pyrrolo[3,2-d]pyrimidin-4-yl)oxy]-phenyl}-3-phenylurea (4)

To a solution of **3** (579 mg, 2.41 mmol), triethylamine (1.00 mL, 7.22 mmol) in THF (10 mL) was added phenyl isocyanate (314 μL, 2.89 mmol), and the mixture was stirred at room temperature for 15 h. The mixture was diluted with AcOEt and washed with water, brine, dried over anhydrous magnesium sulfate, and concentrated under reduced pressure. The residue was purified by basic silica gel column chromatography (AcOEt/hexane) followed by recrystallization from AcOEt–hexane to give **4** (690 mg, 80%) as a white solid: mp 197–199 °C; ¹H NMR (DMSO-d_6) δ 4.10 (3H, s), 6.60–6.61 (1H, m), 6.88–6.98 (2H, m), 7.20–7.30 (3H, m), 7.35 (1H, t, J = 8.1 Hz), 7.43 (2H, d, J = 8.1 Hz), 7.57 (1H, t, J = 2.1 Hz), 7.79 (1H, d, J = 3.0 Hz), 8.29 (1H, s), 8.72 (1H, s), 8.86 (1H, s); Anal. Calcd for C₂₀H₁₇N₅O₂·0.1H₂O: C, 66.51; H, 4.80; N, 19.39. Found: C, 66.35; H, 4.77; N, 19.25.

5.4. N-{3-[(5-Methyl-5H-pyrrolo[3,2-d]pyrimidin-4-yl)oxy]phenyl}-benzamide (5)

To a solution of **3** (415 mg, 1.73 mmol), triethylamine (719 μL, 5.19 mmol) in THF (10 mL) was added benzoyl chloride (221 μL, 1.90 mmol) at 0 °C, and the mixture was stirred at room temperature for 15 h. The mixture was diluted with AcOEt and washed with water, brine, dried over anhydrous magnesium sulfate, and concentrated under reduced pressure. The residue was purified by silica gel column chromatography (AcOEt/hexane) followed by recrystallization from AcOEt–hexane to give **5** (262 mg, 44%) as a white solid: mp 209–212 °C; ¹H NMR (DMSO-d_6) δ 4.12 (3H, s), 6.61 (1H, d, J = 3.0 Hz), 7.04–7.07 (1H, m), 7.44 (1H, t, J = 8.1 Hz), 7.50–7.68 (4H, m), 7.80 (1H, d, J = 3.0 Hz), 7.84 (1H, t, J = 2.3 Hz), 7.93–7.97 (2H, m), 8.30 (1H, s), 10.41 (1H, s); Anal. Calcd for C₂₀H₁₆N₄O₂: C, 69.76; H, 4.68; N, 16.27. Found: C, 69.58; H, 4.53; N, 16.07.

5.5. 4-[(5-Methyl-5H-pyrrolo[3,2-d]pyrimidin-4-yl)oxy]aniline (6)

The compound **6** was prepared from **2** in a manner similar to that described for **3** to yield a pale yellow solid (60%): ¹H NMR (DMSO-d_6) δ 4.06 (3H, s), 5.04 (2H, br s), 6.53 (1H, d, J = 3.0 Hz), 6.58 (2H, d, J = 8.7 Hz), 6.91 (2H, d, J = 8.7 Hz), 7.70 (1H, d, J = 3.0 Hz), 8.21 (1H, s).

5.6. 1-{4-[(5-Methyl-5H-pyrrolo[3,2-d]pyrimidin-4-yl)oxy]-phenyl}-3-phenylurea (7a)

To a solution of **6** (150 mg, 0.624 mmol) in DMF (3 mL) was added N,N′-carbonyldiimidazole (101 mg, 0.624 mmol). After being stirred at room temperature for 1 h, aniline (61.0 mg, 0.655 mmol) was added and the resulting mixture was stirred at room temperature for 15 h. The mixture was diluted with water and extracted with AcOEt. The extract was washed with brine, dried over anhydrous magnesium sulfate, and concentrated under reduced pressure. The residue was purified by basic silica gel column chromatography (AcOEt/hexane) followed by recrystallization from AcOEt–hexane to give **7a** as a white solid: mp 183–186 °C; ¹H NMR (DMSO-d_6) δ 4.04 (3H, s), 6.53 (1H, d, J = 2.9 Hz), 6.90 (1H, t, J = 7.4 Hz), 7.14–7.26 (4H, m), 7.39–7.49 (4H, m), 7.71 (1H, d, J = 2.9 Hz), 8.21 (1H, s), 8.68 (1H, br s), 8.75 (1H, br s); Anal. Calcd for C₂₀H₁₇N₅O₂·0.2H₂O: C, 66.18; H, 4.83; N, 19.29. Found: C, 66.16; H, 4.73; N, 19.23.

The following compounds **7b–h** were prepared using a procedure similar to that described for **7a** from **6**.

5.7. 1-Methyl-3-{4-[(5-methyl-5H-pyrrolo[3,2-d]pyrimidin-4-yl)-oxy]phenyl}urea (7b)

Yield 26%: mp 190–196 °C (AcOEt–hexane); ¹H NMR (DMSO-d_6) δ 2.59 (3H, d, J = 4.8 Hz), 4.03 (3H, s), 5.99 (1H, d, J = 4.8 Hz), 6.51 (1H, d, J = 2.4 Hz), 7.08 (2H, d, J = 8.8 Hz), 7.39 (2H, d, J = 8.8 Hz), 7.70 (1H, d, J = 2.4 Hz), 8.19 (1H, s), 8.54 (1H, br s); Anal. Calcd for C₁₅H₁₅N₅O₂·0.15H₂O: C, 60.05; H, 5.14; N, 23.34. Found: C, 60.16; H, 5.09; N, 23.09.

5.8. 1-{4-[(5-Methyl-5H-pyrrolo[3,2-d]pyrimidin-4-yl)oxy]-phenyl}-3-propylurea (7c)

Yield 17%: mp 184–187 °C (AcOEt–hexane); ¹H NMR (DMSO-d_6) δ 0.86 (3H, t, J = 7.5 Hz), 1.37–1.46 (2H, m), 2.99–3.06 (2H, m), 4.07 (3H, s), 6.15 (1H, t, J = 6.0 Hz), 6.55 (1H, d, J = 3.0 Hz), 7.13 (2H, d, J = 8.7 Hz), 7.43 (2H, d, J = 8.7 Hz), 7.74 (1H, d, J = 3.0 Hz), 8.23 (1H, s), 8.48 (1H, br s); Anal. Calcd for C₁₇H₁₉N₅O₂: C, 62.75; H, 5.89; N, 21.52. Found: C, 62.56; H, 5.75; N, 21.36.

5.9. 1-(2-Chlorophenyl)-3-{4-[(5-methyl-5H-pyrrolo[3,2-d]pyrimidin-4-yl)oxy]phenyl}urea (7d)

Yield 7.0%: mp 196–200 °C (AcOEt–hexane); ¹H NMR (DMSO-d_6) δ 4.05 (3H, s), 6.53 (1H, d, J = 2.9 Hz), 6.94–7.01 (1H, m), 7.16–7.28 (3H, m), 7.38–7.50 (3H, m), 7.72 (1H, d, J = 2.9 Hz), 8.09–8.13 (1H, m), 8.21 (1H, s), 8.32 (1H, br s), 9.56 (1H, br s); Anal. Calcd for C₂₀H₁₆ClN₅O₂·0.2H₂O: C, 60.44; H, 4.16; N, 17.62. Found: C, 60.40; H, 4.15; N, 17.66.

5.10. 1-(3-Chlorophenyl)-3-{4-[(5-methyl-5H-pyrrolo[3,2-d]pyrimidin-4-yl)oxy]phenyl}urea (7e)

Yield 14%: mp 184–186 °C (AcOEt–hexane); ^{1}H NMR (DMSO-d_6) δ 4.04 (3H, s), 6.53 (1H, d, J = 2.8 Hz), 6.94–6.98 (1H, m), 7.15–7.25 (4H, m), 7.46 (2H, d, J = 8.8 Hz), 7.66 (1H, s), 7.71 (1H, d, J = 2.8 Hz), 8.21 (1H, s), 8.78 (1H, br s), 8.85 (1H, br s); Anal. Calcd for $C_{20}H_{16}ClN_5O_2$: C, 60.99; H, 4.09; N, 17.78. Found: C, 60.71; H, 4.21; N, 17.84.

5.11. 1-(4-Chlorophenyl)-3-{4-[(5-methyl-5H-pyrrolo[3,2-d]pyrimidin-4-yl)oxy]phenyl}urea (7f)

Yield 18%: mp 214–218 °C (AcOEt–hexane); ^{1}H NMR (DMSO-d_6) δ 4.04 (3H, s), 6.53 (1H, d, J = 3.1 Hz), 7.16 (2H, d, J = 8.8 Hz), 7.26 (2H, d, J = 8.6 Hz), 7.24–7.48 (4H, m), 7.71 (1H, d, J = 3.1 Hz), 8.21 (1H, s), 8.73 (1H, br s), 8.78 (1H, br s); Anal. Calcd for $C_{20}H_{16}ClN_5O_2$: C, 60.99; H, 4.09; N, 17.78. Found: C, 60.80; H, 4.13; N, 17.83.

5.12. 1-{4-[(5-Methyl-5H-pyrrolo[3,2-d]pyrimidin-4-yl)oxy]phenyl}-3-[3-(trifluoromethyl)phenyl]urea (7g)

Yield 14%: mp 188–190 °C (AcOEt–hexane); ^{1}H NMR (DMSO-d_6) δ 4.04 (3H, s), 6.53 (1H, d, J = 2.8 Hz), 7.15–7.27 (3H, m), 7.41–7.51 (4H, m), 7.71 (1H, d, J = 2.8 Hz), 7.98 (1H, s), 8.21 (1H, s), 8.94 (1H, br s), 9.14 (1H, br s); Anal. Calcd for $C_{21}H_{16}F_3N_5O_2$: C, 59.02; H, 3.77; N, 16.39. Found: C, 58.77; H, 3.74; N, 16.22.

5.13. 1-(3-Bromophenyl)-3-{4-[(5-methyl-5H-pyrrolo[3,2-d]pyrimidin-4-yl)oxy]phenyl}urea (7h)

Yield 16%: mp 207–211 °C (AcOEt–hexane); ^{1}H NMR (DMSO-d_6) δ 4.08 (3H, s), 6.57 (1H, d, J = 3.0 Hz), 7.13 (1H, d, J = 8.0 Hz), 7.20–7.24 (3H, m), 7.31 (1H, d, J = 8.0 Hz), 7.51 (2H, d, J = 9.0 Hz), 7.75 (1H, d, J = 3.0 Hz), 7.85 (1H, t, J = 2.1 Hz), 8.25 (1H, s), 8.88 (1H, br s), 8.95 (1H, br s); Anal. Calcd for $C_{20}H_{16}BrN_5O_2$: C, 54.81; H, 3.68; N, 15.98. Found: C, 54.76; H, 3.71; N, 15.84.

5.14. 1-(3-Fluorophenyl)-3-{4-[(5-methyl-5H-pyrrolo[3,2-d]pyrimidin-4-yl)oxy]phenyl}urea (7i)

The compound 7i was prepared from 6 in a manner similar to that described for 4 to yield a white solid (59%): mp 189–191 °C (AcOEt–hexane); ^{1}H NMR (DMSO-d_6) δ 4.08 (3H, s), 6.56–6.57 (1H, m), 6.73–6.57 (1H, m), 7.10–7.13 (1H, m), 7.20–7.32 (3H, m), 7.46–7.52 (3H, m), 7.75 (1H, d, J = 3.3 Hz), 8.25 (1H, s), 8.81 (1H, s), 8.91 (1H, br s); Anal. Calcd for $C_{20}H_{16}FN_5O_2$: C, 63.65; H, 4.27; N, 18.56. Found: C, 63.54; H, 4.11; N, 18.49.

5.15. 1-(3-Methylphenyl)-3-{4-[(5-methyl-5H-pyrrolo[3,2-d]pyrimidin-4-yl)oxy]phenyl}urea (7j)

The compound 7j was prepared from 6 in a manner similar to that described for 4 to yield a white solid (76%): mp 174–176 °C (AcOEt–hexane); ^{1}H NMR (DMSO-d_6) δ 2.26 (3H, s), 4.09 (3H, s), 6.57 (1H, d, J = 3.2 Hz), 6.77 (1H, d, J = 7.2 Hz), 7.11–7.29 (5H, m), 7.48–7.51 (2H, m), 7.75 (1H, d, J = 3.2 Hz), 8.25 (1H, s), 8.59 (1H, s), 8.71 (1H, br s); Anal. Calcd for $C_{21}H_{19}N_5O_2$: C, 67.55; H, 5.13; N, 18.76. Found: C, 67.32; H, 5.17; N, 18.50.

5.16. N-{4-[(5-Methyl-5H-pyrrolo[3,2-d]pyrimidin-4-yl)oxy]phenyl}benzamide (8)

The compound 8 was prepared from 6 in a manner similar to that described for 5 to yield a white solid (7.6%): mp 209–212 °C (AcOEt–hexane); ^{1}H NMR (DMSO-d_6) δ 4.12 (3H, s), 6.59–6.60

(1H, m), 7.30 (2H, d, J = 8.7 Hz), 7.52–7.63 (3H, m), 7.79 (1H, d, J = 3.0 Hz), 7.85 (2H, d, J = 8.7 Hz), 7.98 (2H, d, J = 7.5 Hz), 8.28 (1H, s), 10.36 (1H, s); Anal. Calcd for $C_{20}H_{16}N_4O_2 \cdot 0.1H_2O$: C, 69.39; H, 4.72; N, 16.18. Found: C, 69.15; H, 4.59; N, 16.40.

5.17. N-{4-[(5-Methyl-5H-pyrrolo[3,2-d]pyrimidin-4-yl)oxy]phenyl}-2-phenylacetamide (9)

The compound 9 was prepared from 6 in a manner similar to that described for 5 to yield a white solid (84%): mp 164–165 °C (AcOEt–hexane); ^{1}H NMR (DMSO-d_6) δ 3.66 (2H, s), 4.09 (3H, s), 6.58 (1H, d, J = 3.0 Hz), 7.22–7.38 (7H, m), 7.67 (2H, d, J = 9.0 Hz), 7.77 (1H, d, J = 3.0 Hz), 8.26 (1H, s), 10.26 (1H, br s); Anal. Calcd for $C_{21}H_{18}N_4O_2 \cdot 0.2H_2O$: C, 69.68; H, 5.12; N, 15.48. Found: C, 69.80; H, 5.15; N, 15.20.

5.18. 1-{4-[(5-Methyl-5H-pyrrolo[3,2-d]pyrimidin-4-yl)oxy]phenyl}-3-phenylthiourea (10)

To a solution of 6 (1.10 g, 4.58 mmol), triethylamine (1.90 mL, 13.7 mmol) in THF (10 mL) was added phenyl isothiocyanate (657 μL, 5.44 mmol), and the mixture was stirred at room temperature for 15 h. The mixture was diluted with AcOEt and washed with water, brine, dried over anhydrous magnesium sulfate, and concentrated under reduced pressure. The residue was purified by basic silica gel column chromatography (AcOEt/hexane) followed by recrystallization from AcOEt–hexane to give 10 (1.29 g, 75%) as a white solid: mp 155–157 °C; ^{1}H NMR (DMSO-d_6) δ 4.11 (3H, s), 6.60 (1H, d, J = 3.2 Hz), 7.10–7.16 (1H, m), 7.24–7.38 (4H, m), 7.47–7.58 (4H, m), 7.78 (1H, d, J = 3.2 Hz), 8.29 (1H, s), 9.84 (2H, s); Anal. Calcd for $C_{20}H_{17}N_5OS$: C, 63.98; H, 4.56; N, 18.65. Found: C, 63.67; H, 4.60; N, 18.52.

5.19. N-{4-[(5-Methyl-5H-pyrrolo[3,2-d]pyrimidin-4-yl)oxy]phenyl}-1H-benzimidazol-2-amine (11)

A mixture of 6 (475 mg, 1.98 mmol), 2-chloro-1H-benzimidazole (322 mg, 2.18 mmol), and NMP (5 mL) was stirred at 120 °C for 15 h. The mixture was diluted with water and extracted with AcOEt. The extract was washed with brine, dried over anhydrous magnesium sulfate, and concentrated under reduced pressure. The residue was purified by silica gel column chromatography (AcOEt/hexane) followed by recrystallization from AcOEt–hexane to give 11 (66.0 mg, 9.3%) as a white solid: mp 219–222 °C; ^{1}H NMR (DMSO-d_6) δ 4.12 (3H, s), 6.59 (1H, d, J = 3.0 Hz), 6.94–7.04 (2H, m), 7.22–7.38 (4H, m), 7.77 (1H, d, J = 3.0 Hz), 7.83 (2H, d, J = 9.0 Hz), 8.27 (1H, s), 9.52 (1H, s), 10.97 (1H, s); Anal. Calcd for $C_{20}H_{16}N_6O$: C, 67.40; H, 4.53; N, 23.58. Found: C, 67.11; H, 4.43; N, 23.52.

5.20. 3-[(5-Methyl-5H-pyrrolo[3,2-d]pyrimidin-4-yl)oxy]benzoic acid (12a)

A mixture of 2 (2.23 g, 13.3 mmol), 3-hydroxybenzoic acid (2.02 g, 14.6 mmol), cesium carbonate (13.0 g, 39.9 mmol), and DMSO (20 mL) was stirred at 100 °C for 4 h. The mixture was acidified with 1 M HCl and the resulting solid was collected to give 12a (3.48 g, 76%) as a white solid: ^{1}H NMR (DMSO-d_6) δ 4.12 (3H, s), 6.62 (1H, d, J = 3.0 Hz), 7.58–7.64 (2H, m), 7.80–7.91 (3H, m), 8.30 (1H, s), 13.21 (1H, br s).

5.21. 4-[(5-Methyl-5H-pyrrolo[3,2-d]pyrimidin-4-yl)oxy]benzoic acid (12b)

The compound 12b was prepared from 2 in a manner similar to that described for 12a to yield a white solid (72%): ^{1}H NMR (DMSO-

d_6) δ 4.10 (3H, s), 6.62 (1H, d, J = 3.3 Hz), 7.44 (2H, d, J = 8.9 Hz), 7.81 (1H, d, J = 3.3 Hz), 8.04 (2H, d, J = 8.9 Hz), 8.31 (1H, s), 13.02 (1H, br s).

5.22. 3-[(5-Methyl-5*H*-pyrrolo[3,2-*d*]pyrimidin-4-yl)oxy]-*N*-phenylbenzamide (13a)

To a solution of **12a** (552 mg, 2.05 mmol), 1-hydroxybenzotriazole (415 mg, 2.05 mg), and aniline (187 μL, 2.05 mmol) in DMF (5 mL) was added 1-ethyl-3-(3-dimethylaminopropyl) carbodiimide hydrochloride (589 mg, 3.07 mmol) at 0 °C, and the mixture was stirred at room temperature for 15 h. The mixture was diluted with water and extracted with AcOEt. The extract was washed with brine, dried over anhydrous magnesium sulfate, and concentrated under reduced pressure. The residue was purified by basic silica gel column chromatography (AcOEt/hexane) followed by recrystallization from AcOEt–hexane to give **13a** (496 mg, 70%) as a white solid: mp 223–228 °C; ^{1}H NMR (DMSO-d_6) δ 4.14 (3H, s), 6.62 (1H, d, J = 3.0 Hz), 7.07–7.13 (1H, m), 7.32–7.38 (2H, m), 7.54–7.67 (2H, m), 7.75–7.82 (3H, m), 7.89–7.92 (2H, m), 8.30 (1H, s), 10.31 (1H, s); Anal. Calcd for $C_{20}H_{16}N_4O_2$: C, 69.76; H, 4.68; N, 16.27. Found: C, 69.48; H, 4.59; N, 16.03.

5.23. 4-[(5-Methyl-5*H*-pyrrolo[3,2-*d*]pyrimidin-4-yl)oxy]-*N*-phenylbenzamide (13b)

The compound **13b** was prepared from **12b** in a manner similar to that described for **3** to yield a white solid (28%): mp 157–160 °C (AcOEt–hexane); ^{1}H NMR (DMSO-d_6) δ 4.12 (3H, s), 6.62 (1H, d, J = 3.0 Hz), 7.10 (1H, t, J = 7.7 Hz), 7.36 (2H, t, J = 7.7 Hz), 7.48 (2H, d, J = 8.6 Hz), 7.78–7.83 (3H, m), 8.06 (2H, d, J = 8.6 Hz), 8.31 (1H, s), 10.30 (1H, s); Anal. Calcd for $C_{20}H_{16}N_4O_2$: C, 69.76; H, 4.68; N, 16.27. Found: C, 69.74; H, 4.63; N, 16.34.

5.24. Ethyl {4-[(5-methyl-5*H*-pyrrolo[3,2-*d*]pyrimidin-4-yl)oxy]-phenyl}acetate (14)

The compound **14** was prepared from **2** in a manner similar to that described for **12a** to yield a white solid (88%): ^{1}H NMR (DMSO-d_6) δ 1.28 (3H, t, J = 7.2 Hz), 3.65 (2H, s), 4.14 (3H, s), 4.17 (2H, q, J = 7.2 Hz), 6.65 (1H, d, J = 3.0 Hz), 7.22 (2H, d, J = 8.4 Hz), 7.32 (1H, d, J = 3.0 Hz), 7.39 (2H, d, J = 8.4 Hz), 8.44 (1H, s).

5.25. {4-[(5-Methyl-5*H*-pyrrolo[3,2-*d*]pyrimidin-4-yl)oxy]-phenyl}acetic acid (15)

A mixture of **14** (990 mg, 3.2 mmol), 8 M NaOH (1 mL), and MeOH (10 mL) was stirred at room temperature for 18 h. The mixture was acidified with 1 M HCl and the resulting solid was collected followed by recrystallization from MeOH to give **15** (669 mg, 74%) as a white solid: ^{1}H NMR (DMSO-d_6) δ 3.62 (2H, s), 4.10 (3H, s), 6.59 (1H, d, J = 3.2 Hz), 7.25 (2H, d, J = 8.6 Hz), 7.35 (2H, d, J = 8.6 Hz), 7.78 (1H, d, J = 3.2 Hz), 8.28 (1H, s), 12.37 (1H, br s).

5.26. 2-{4-[(5-Methyl-5*H*-pyrrolo[3,2-*d*]pyrimidin-4-yl)oxy]-phenyl}-*N*-phenylacetamide (16)

The compound **16** was prepared from **15** in a manner similar to that described for **13a** to yield a white solid (81%): mp 236–240 °C (AcOEt–hexane); ^{1}H NMR (DMSO-d_6) δ 3.69 (2H, s), 4.10 (3H, s), 6.59 (1H, d, J = 3.0 Hz), 7.05 (1H, t, J = 7.5 Hz), 7.26 (2H, d, J = 8.7 Hz), 7.32 (2H, d, J = 7.5 Hz), 7.42 (2H, d, J = 8.7 Hz), 7.61 (2H, d, J = 7.5 Hz), 7.78 (1H, d, J = 3.0 Hz), 8.27 (1H, s), 10.18 (1H, br s); Anal. Calcd for $C_{21}H_{18}N_4O_2$: C, 70.38; H, 5.06; N, 15.63. Found: C, 70.21; H, 5.02; N, 15.70.

5.27. 4-[(5-Methyl-5*H*-pyrrolo[3,2-*d*]pyrimidin-4-yl)sulfanyl]-aniline (17a)

The compound **17a** was prepared from **2** in a manner similar to that described for **3** to yield a white solid (39%): ^{1}H NMR (DMSO-d_6) δ 4.16 (3H, s), 5.56 (2H, s), 6.52 (1H,d, J = 3.0 Hz), 6.62 (2H, d, J = 8.7 Hz), 7.19 (2H, d, J = 8.7 Hz), 7.74 (1H, d, J = 3.0 Hz), 8.37 (1H, s).

5.28. *N*-(5-Methyl-5*H*-pyrrolo[3,2-*d*]pyrimidin-4-yl)benzene-1,4-diamine (17b)

A mixture of **2** (2.06 g, 12.3 mmol), 4-nitroaniline (2.04 g, 14.7 mmol), 4 M HCl in AcOEt (5.5 mL), and 2-propanol (10 mL) was stirred at 80 °C for 1 h. The mixture was diluted with AcOEt and washed with water, brine, dried over anhydrous magnesium sulfate, and concentrated under reduced pressure. The residue was dissolved in MeOH (10 mL) and 10% palladium on carbon (water ~50%, 100 mg) was added. The resulting mixture was stirred under a hydrogen atmosphere at room temperature for 3 h. The catalyst was filtered off, and the filtrate was concentrated in vacuo. The residual solid was collected and washed with AcOEt–hexane to give **17b** (867 mg, 88%) as a white solid: ^{1}H NMR (DMSO-d_6) δ 4.10 (3H, s), 4.90 (2H, s), 6.33 (1H, d, J = 3.0 Hz), 6.55 (2H, d, J = 8.4 Hz), 7.17 (2H, d, J = 8.4 Hz), 7.44 (1H, d, J = 3.0 Hz), 7.99 (1H, s), 8.08 (1H, s).

5.29. *N*-Methyl-*N*-(5-methyl-5*H*-pyrrolo[3,2-*d*]pyrimidin-4-yl)-benzene-1,4-diamine (17c)

To a suspension of sodium hydride (60% in oil, 300 mg, 7.5 mmol) in DMF (10 mL) was added *N*-methyl-4-nitroaniline (761 mg, 5.0 mmol) at 0 °C, and the mixture was stirred. After 30 min, **2** was added to the mixture, and the resulting mixture was stirred at room temperature for 18 h. The mixture was diluted with AcOEt and washed with water, brine, dried over anhydrous magnesium sulfate, and concentrated under reduced pressure. The residue was purified by silica gel column chromatography (AcOEt/hexane) to give a yellow solid. The solid thus obtained was dissolved in MeOH (30 mL) and 10% palladium on carbon (water ~50%, 162 mg) was added. The resulting mixture was stirred under a hydrogen atmosphere at room temperature for 6 h. The catalyst was filtered off, and the filtrate was concentrated in vacuo. The residue was purified by basic silica gel column chromatography (AcOEt/hexane). The residual solid was collected and washed with AcOEt–hexane to give **17c** (328 mg, 1.29 mmol, 91%) as a white solid: ^{1}H NMR (DMSO-d_6) δ 3.08 (3H, s), 3.36 (3H, s), 5.06 (2H, s), 6.39 (1H, d, J = 3.0 Hz), 6.51 (2H, d, J = 8.7 Hz), 6.68 (2H, d, J = 8.7 Hz), 7.36 (1H, d, J = 3.0 Hz), 8.39 (1H, s).

5.30. 1-{4-[(5-Methyl-5*H*-pyrrolo[3,2-*d*]pyrimidin-4-yl)sulfanyl]-phenyl}-3-phenylurea (18a)

The compound **18a** was prepared from **17a** in a manner similar to that described for **4** to yield a white solid (75%): mp 204–207 °C (AcOEt–hexane); ^{1}H NMR (DMSO-d_6) δ 4.19 (3H, s), 6.55 (1H, d, J = 3.0 Hz), 6.95–7.01 (1H, m), 7.26–7.32 (2H, m), 7.45–7.60 (6H, m), 7.79 (1H, d, J = 3.0 Hz), 8.40 (1H, s), 8.78 (1H, s), 8.94 (1H, s); Anal. Calcd for $C_{20}H_{79}N_5OS$: C, 63.98; H, 4.56; N, 18.65. Found: C, 64.11; H, 4.53; N, 18.63.

5.31. 1-{4-[(5-Methyl-5*H*-pyrrolo[3,2-*d*]pyrimidin-4-yl)amino]-phenyl}-3-phenylurea (18b)

The compound **18b** was prepared from **17b** in a manner similar to that described for **4** to yield a white solid (13%): mp 207–210 °C

(AcOEt–hexane); ^{1}H NMR (DMSO-d_6) δ 4.14 (3H, s), 6.40 (1H, d, J = 3.3 Hz), 6.92–6.99 (1H, m), 7.24–7.56 (8H, m), 8.20 (1H, s), 8.29 (1H, s), 8.55–8.66 (3H, m); Anal. Calcd for $C_{20}H_{18}N_6O\cdot0.5H_2O$: C, 65.38; H, 5.21; N, 22.87. Found: C, 65.59; H, 5.01; N, 22.87.

5.32. 1-{4-[[Methyl(5-methyl-5H-pyrrolo[3,2-d]pyrimidin-4-yl)-amino]phenyl}-3-[3-(trifluoromethyl)phenyl]urea (18c)

The compound **18c** was prepared from **17c** in a manner similar to that described for **4** to yield a white solid (80%): mp 170–174 °C (AcOEt–hexane); ^{1}H NMR (DMSO-d_6) δ 3.18 (3H, s), 3.47 (3H, s), 6.48 (1H, d, J = 3.0 Hz), 6.88 (2H, d, J = 8.9 Hz), 7.30 (1H, d, J = 7.5 Hz), 7.40 (2H, d, J = 8.9 Hz), 7.45–7.65 (3H, m), 8.01 (1H, s), 8.50 (1H, s), 8.80 (1H, s), 9.03 (1H, s); Anal. Calcd for $C_{22}H_{19}F_3N_6O$: C, 60.00; H, 4.35; N, 19.08. Found: C, 59.99; H, 4.30; N, 18.92.

5.33. 2-Chloro-4-[(5-methyl-5H-pyrrolo[3,2-d]pyrimidin-4-yl)-oxy]aniline (19a)

A mixture of **2** (168 mg, 1.0 mmol), 4-amino-3-chlorophenol (215 mg, 1.5 mmol), potassium carbonate (415 mg, 3.0 mmol), and NMP (3 mL) was stirred at 120 °C for 18 h. The mixture was diluted with water and extracted with AcOEt. The extract was washed with brine, dried over anhydrous magnesium sulfate, and concentrated under reduced pressure. The residue was purified by basic silica gel column chromatography (AcOEt/hexane) to give **19a** (100 mg, 36%) as a white solid: ^{1}H NMR (DMSO-d_6) δ 4.05 (2H, br s), 4.13 (3H, s), 6.64 (1H, d, J = 3.0 Hz), 6.84 (1H, d, J = 8.7 Hz), 7.00 (1H, dd, J = 8.7, 2.4 Hz), 7.20 (1H, d, J = 2.4 Hz), 7.31 (1H, d, J = 3.0 Hz), 8.45 (1H, s).

5.34. 3-Chloro-4-[(5-methyl-5H-pyrrolo[3,2-d]pyrimidin-4-yl)-oxy]aniline (19b)

The compound **19b** was prepared from **2** in a manner similar to that described for **19a** to yield a white solid (32%): ^{1}H NMR (DMSO-d_6) δ 4.07 (3H, s), 5.35 (2H, br s), 6.56–6.58 (2H, m), 6.69–6.70 (1H, m), 7.07 (1H, d, J = 8.7 Hz), 7.74 (1H, d, J = 2.7 Hz), 8.22 (1H, s).

5.35. 2-Methoxy-4-[(5-methyl-5H-pyrrolo[3,2-d]pyrimidin-4-yl)-oxy]aniline (19c)

The compound **19c** was prepared from **2** in a manner similar to that described for **19a** to yield a white solid (61%): ^{1}H NMR (DMSO-d_6) δ 3.74 (3H, s), 4.08 (3H, s), 4.67 (2H, s), 6.55–6.67 (3H, m), 6.78 (1H, d, J = 2.1 Hz), 7.73 (1H, d, J = 3.0 Hz), 8.24 (1H, s).

5.36. 2-Fluoro-4-[(5-methyl-5H-pyrrolo[3,2-d]pyrimidin-4-yl)-oxy]aniline (19d)

A mixture of **2** (550 mg, 3.28 mmol), 3-fluoro-4-nitrophenol (619 mg, 3.94 mmol), and *o*-xylene (20 mL) was stirred at 100 °C for 48 h. The mixture was diluted with AcOEt and washed with water, brine, dried over anhydrous magnesium sulfate, and concentrated under reduced pressure. The residual solid was collected and washed with AcOEt–hexane to give 4-(3-fluoro-4-nitrophen-oxy)-5-methyl-5H-pyrrolo[3,2-d] pyrimidine (725 mg, 77%) as a white solid. A mixture of 4-(3-fluoro-4-nitrophenoxy)-5-methyl-5H-pyrrolo[3,2-d] pyrimidine (715 mg, 0.867 mmol), zinc (1.62 g, 24.8 mmol), ammonium chloride (531 mg, 9.92 mmol) and MeOH (10 mL) was stirred at reflux for 1 h. The mixture was filtered through Celite, and the filtrate was concentrated under reduced pressure. The residual solid was collected and washed with AcOEt–hexane to give **19d** (256 mg, 40%) as a white solid: ^{1}H NMR (DMSO-d_6) δ 4.08 (3H, s), 5.11 (2H, s), 6.57 (1H, d,

J = 3.2 Hz), 6.77–6.89 (2H, m), 7.05 (1H, dd, J = 12.0, 2.1 Hz), 7.75 (1H, d, J = 3.2 Hz), 8.26 (1H, s).

5.37. 1-{2-Chloro-4-[(5-methyl-5H-pyrrolo[3,2-d]pyrimidin-4-yl)-oxy]phenyl}-3-[3-(trifluoromethyl)phenyl]urea (20a)

The compound **20a** was prepared from **19a** in a manner similar to that described for **4** to yield a white solid (61%): mp 192–194 °C (AcOEt–hexane); ^{1}H NMR (DMSO-d_6) δ 4.11 (3H, s), 6.61 (1H, d, J = 3.0 Hz), 7.30–7.36 (2H, m), 7.52–7.58 (3H, m), 7.80 (1H, d, J = 3.0 Hz), 8.06 (1H, br s), 8.18 (1H, d, J = 8.7 Hz), 8.31 (1H, s), 8.45 (1H, br s), 9.73 (1H, br s); Anal. Calcd for $C_{21}H_{15}ClF_3N_5O_2$: C, 54.61; H, 3.27; N, 15.16. Found: C, 54.53; H, 3.25; N, 15.17.

5.38. 1-{3-Chloro-4-[(5-methyl-5H-pyrrolo[3,2-d]pyrimidin-4-yl)-oxy]phenyl}-3-[3-(trifluoromethyl)phenyl]urea (20b)

The compound **20b** was prepared from **19b** in a manner similar to that described for **4** to yield a white solid (85%): mp 241–242 °C (AcOEt–hexane); ^{1}H NMR (DMSO-d_6) δ 4.10 (3H, s), 6.59–6.60 (1H, m), 7.31 (1H, d, J = 8.0 Hz), 7.37–7.43 (2H, m), 7.51 (1H, t, J = 8.0 Hz), 7.59 (1H, d, J = 8.7 Hz), 7.79 (1H, d, J = 3.3 Hz), 7.84–7.85 (1H, m), 8.01 (1H, s), 8.25 (1H, s), 9.06 (1H, s), 9.16 (1H, br s); Anal. Calcd for $C_{21}H_{15}ClF_3N_5O_2$: C, 54.61; H, 3.27; N, 15.16. Found: C, 54.59; H, 3.29; N, 15.03.

5.39. 1-{2-Methoxy-4-[(5-methyl-5H-pyrrolo[3,2-d]pyrimidin-4-yl)oxy]phenyl}-3-[3-(trifluoromethyl)phenyl]urea (20c)

The compound **20c** was prepared from **19c** in a manner similar to that described for **4** to yield a white solid (54%): mp 173–177 °C (AcOEt–hexane); ^{1}H NMR (DMSO-d_6) δ 3.38 (3H, s), 4.12 (3H, s), 6.60 (1H, d, J = 3.3 Hz), 6.86 (1H, dd, J = 8.9, 2.3 Hz), 7.07 (1H, d, J = 2.3 Hz), 7.30–7.34 (1H, m), 7.52–7.54 (2H, m), 7.78 (1H, d, J = 3.3 Hz), 8.06 (1H, s), 8.15 (1H, d, J = 8.9 Hz), 8.29 (1H, s), 8.33 (1H, s), 9.67 (1H, s); Anal. Calcd for $C_{22}H_{18}F_3N_5O_3\cdot0.2H_2O$: C, 57.32; H, 4.02; N, 15.19. Found: C, 57.22; H, 3.85; N, 15.12.

5.40. 1-{2-Fluoro-4-[(5-methyl-5H-pyrrolo[3,2-d]pyrimidin-4-yl)-oxy]phenyl}-3-[3-(trifluoromethyl)phenyl]urea (20d)

The compound **20d** was prepared from **19d** in a manner similar to that described for **4** to yield a white solid (87%): mp 196–198 °C (AcOEt–hexane); ^{1}H NMR (DMSO-d_6) δ 4.10 (3H, s), 6.61 (1H, d, J = 3.0 Hz), 7.12–7.19 (1H, m), 7.30–7.44 (2H, m), 7.50–7.60 (2H, m), 7.79 (1H, d, J = 3.0 Hz), 8.05 (1H, s), 8.13 (1H, t, J = 9.3 Hz), 8.30 (1H, s), 8.67 (1H, s), 9.41 (1H, s); Anal. Calcd for $C_{21}H_{15}F_4N_5O_2$: C, 56.63; H, 3.39; N, 15.72. Found: C, 56.62; H, 3.24; N, 15.78.

5.41. 4-Chloro-5-(2-chloroethyl)-5H-pyrrolo[3,2-d]pyrimidine (21)

The compound **21** was prepared from **1** in a manner similar to that described for **2** to yield a white solid (54%): ^{1}H NMR (DMSO-d_6) δ 4.10 (2H, t, J = 5.9 Hz), 4.72 (2H, t, J = 5.9 Hz), 6.51 (1H, d, J = 3.0 Hz), 7.22 (1H, d, J = 3.0 Hz), 8.75 (1H, s).

5.42. 1-(4-{[5-(2-Chloroethyl)-5H-pyrrolo[3,2-d]pyrimidin-4-yl]-amino}phenyl)-3-[3-(trifluoromethyl)phenyl]urea (22)

A mixture of **21** (318 mg, 1.47 mmol), **25** (493 mg, 1.49 mmol), and 2-propanol (10 mL) was stirred at 80 °C for 1 h. The mixture was diluted with AcOEt and washed with water, brine, dried over anhydrous magnesium sulfate, and concentrated under reduced pressure. The residue was purified by basic silica gel column chromatography (AcOEt/MeOH) to give **22** (466 mg, 67%) as a white solid: ^{1}H NMR (DMSO-d_6) δ 4.28–4.32 (2H, m), 4.48–4.53 (2H, m),

6.58 (1H, d, *J* = 2.9 Hz), 7.32–7.59 (8H, m), 7.82 (1H, d, *J* = 2.9 Hz), 8.02 (1H, s), 8.49 (1H, s), 9.26 (1H, s), 9.44 (1H, s).

5.43. 1-[4-(5,6-Dihydro-4*H*-pyrrolo[3,2,1-*de*]pteridin-4-yl)-phenyl]-3-[3-(trifluoromethyl)phenyl]urea (23)

A mixture of **22** (450 mg, 0.948 mmol), potassium carbonate (392 mg, 2.84 mmol), and DMF (10 mL) was stirred at 80 °C for 15 h. The mixture was diluted with AcOEt and washed with water, brine, dried over anhydrous magnesium sulfate, and concentrated under reduced pressure. The residue was purified by basic silica gel column chromatography (AcOEt) followed by recrystallization from AcOEt–hexane to give **23** (260 mg, 63%) as a white solid: mp 197–200 °C; ¹H NMR (DMSO-*d₆*) δ 4.16–4.20 (2H, m), 4.39–4.43 (2H, m), 6.45 (1H, d, *J* = 2.7 Hz), 7.31 (1H, d, *J* = 7.5 Hz), 7.43–7.60 (7H, m), 8.03 (1H, s), 8.20 (1H, m), 8.89 (1H, s), 9.09 (1H, s); Anal. Calcd for $C_{22}H_{17}F_3N_6O$: C, 60.27; H, 3.91; N, 19.17. Found: C, 60.17; H, 3.80; N, 19.21.

5.44. 1-(4-Aminophenyl)-3-[3-(trifluoromethyl)phenyl]urea hydrochloride (25)

To a solution of 4-nitroaniline (2.02 g, 14.6 mmol), triethylamine (6.07 mL, 43.8 mmol) in THF (10 mL) was added 3-(trifluoromethyl)phenyl isocyanate (2.45 mL, 17.5 mmol), and the mixture was stirred at room temperature for 15 h. The mixture was diluted with AcOEt and washed with water, brine, dried over anhydrous magnesium sulfate, and concentrated under reduced pressure. The residue was dissolved in MeOH (10 mL) and 10% palladium on carbon (water ∼50%, 100 mg) was added. The resulting mixture was stirred under a hydrogen atmosphere at room temperature for 3 h. The catalyst was filtered off, and 4 M HCl/AcOEt (4 mL) was added to the filtrate. The resulting solid was collected and washed with AcOEt–hexane to give **25** (1.42 g, 29%) as a white solid: ¹H NMR (DMSO-*d₆*) δ 7.26–7.32 (3H, s), 7.47–7.59 (4H, m), 8.00 (1H, s), 9.49 (1H, s), 9.65 (1H, s), 9.93 (3H, br s).

5.45. Docking model of VEGFR2

Pyrrolo[3,2-*d*]pyrimidine derivative (A) was docked into the crystal structure of VEGFR2 (PDB ID: 1VR2) by using GOLD (version 3.2, 2007, The Cambridge Crystallographic Data Centre, UK). After docking calculation, obtained complex model structure was energetically optimized on MOE platform (version 2006.0804, 2006, Chemical Computing Group, Canada). Optimization was performed on the following conditions: MMFF94s for force field setting, 4 × *r* (*r* = interatomic distance) for the dielectric constant setting, AMBER99 for the partial charge setting for all atoms of protein, and AM1-BCC for the partial charge setting for ligand.

5.46. Expression, purification, crystallization and structure determination

The gene for human VEGFR2 (residue 806–1171 except a kinase insertion domain (KID) region (940–989)) was cloned into a pFast-BacHT (Invitrogen, USA) baculovirus expression vector with an N-terminal 6-Histidine tag containing an recombinant Tobacco Etch Virus (rTEV) protease cleavage site. The protein was expressed in Sf9 insect cells (Invitrogen) and purified by immobilized metal-chelate affinity chromatography (IMAC). Protein bound to the IMAC column was eluted with a buffer containing 20 mM Tris–HCl pH 8.0, 0.5 M NaCl, 10% glycerol, 5 mM DTT and 250 mM imidazole. The eluent from the IMAC column was loaded onto a Sephacryl S-200 size exclusion column pre-equilibrated in 20 mM Tris–HCl pH 8.0, 50 mM NaCl, 5 mM DTT and 10% glycerol and eluted with the same buffer. Fractions containing the monomeric protein species were

pooled and then the tag was removed by cleavage with rTEV protease, followed by a Mono-Q anion exchange column pre-equilibrated in 20 mM Tris–HCl pH 8.0, 50 mM NaCl and 5 mM DTT and eluted using a linear gradient to 20 mM Tris–HCl pH 8.0, 300 mM NaCl and 5 mM DTT. Fractions containing the non-phosphorylated protein species were pooled and exchanged its buffer to 50 mM HEPES pH 7.5, 25 mM NaCl, 10 mM DTT and 10% glycerol by a HiPrep desalting column. Inhibitor in DMSO solution was added to a solution of approximately 8 mg/mL protein with gentle stirring to give a final concentration of 0.5 mM, and the enzyme–inhibitor complex was then incubated for 3 h on ice.

Crystallization experiments were performed at 4 °C by mixing 100 nL of enzyme/inhibitor (**20d**) solution with 100 nL of precipitant solution containing 1.3 M tri-sodium citrate. Crystals were harvested by mixing precipitant solution with the cryoprotectant glycerol to a final concentration of 24% and flash-frozen by direct immersion in liquid nitrogen. X-ray diffraction data of the crystals were collected at 100 K with RIGAKU in-house CuKα X-ray generator and RAXIS image-plate system, and at SPring-8 in Harima, Japan on beam-line BL32B2 at a wavelength of 1 Å, respectively. The crystals belong to the monoclinic space group *C*2 with approximate cell dimensions 135 × 56 × 52 Å, β = 95°, diffracting to 1.55 Å resolution. The structure was solved by molecular replacement with MOLREP in the CCP4 program suite using the apo structure of VEGFR2 and refined with CNX2002. The final refined crystallographic statistics for the co-crystal structure with **20d** are *R* = 18.6% (*R*ₓfree = 20.9%) with root-mean-square deviations (RMSD) in bond lengths and angles of 0.007 Å and 1.2°, respectively.

5.47. Measurement of inhibitory activities against VEGFR2, PDGFRβ and FGFR1 kinases

VEGFR2, PDGFRβ and FGFR1 kinase activities were determined by use of an anti-phosphotyrosine antibody with quantitation performed through the AlphaScreen® system (PerkinElmer, USA). For VEGFR2, enzyme reactions were performed in 50 mM Tris–HCl pH 7.5, 5 mM MnCl₂, 5 mM MgCl₂, 0.01% Tween-20 and 2 mM DTT, containing 10 μM ATP, 0.1 μg/mL biotinylated poly-GluTyr (4:1) and 0.1 nM of VEGFR2 (Millipore, UK). For PDGFRβ, the kinase assay was performed as described above with 0.8 nM of PDGFRβ (Millipore) and 20 μM of ATP. For FGFR1, kinase assay was performed as described above with 0.1 nM of FGFR1 (ProQinase GmbH, Germany) and 0.2 μM of ATP.

Prior to catalytic initiation with ATP, compound and enzyme were incubated for 5 min at room temperature. The reactions were quenched by the addition of 25 μL of 100 mM EDTA, 10 μg/mL AlphaScreen streptavidine donor beads and 10 μg/mL acceptor beads in 62.5 mM HEPES pH 7.4, 250 mM NaCl, and 0.1% BSA. Plates were incubated in the dark overnight and then read by EnVision 2102 Multilabel Reader (PerkinElmer). Wells containing the substrate and the enzyme without compound were used as total reaction control. Wells containing biotinylated poly-GluTyr (4:1) and enzyme without ATP were used as basal control. The concentration of inhibitor producing 50% inhibition of the kinase activities (IC₅₀ values) and 95% confidence intervals (95% CI) for VEGFR2, PDGFRβ and FGFR1 were analyzed using GraphPad Prism version 5.01, GraphPad Software (USA). Sigmoidal dose–response (variable slope) curves were fitted using non-linear regression analysis, with the top and bottom of the curve constrained at 100 and 0, respectively.

5.48. Dilution assay of VEGFR2-20d complex

To confirm slow dissociative property of the compound, enzyme–inhibitor dilution assay was performed.[26,27] The recovery of enzyme activity from a preformed enzyme–inhibitor complex

was measured using the AlphaScreen® system as described above. VEGFR2 at 100-fold higher concentration than the standard reaction condition (Section 5.46) and **20d** at 10-fold higher concentration than IC$_{50}$ value were incubated together in reaction buffer for 60 min at ambient temperature to form enzyme–inhibitor complex. This complex was diluted 1:100 into reaction buffer containing 1 mM ATP and 0.1 μg/mL biotinylated poly-GluTyr (4:1), to initiate the kinase reaction.

5.49. Kinase profiling by IC$_{50}$ measurement

Kinase profiling was performed as described previously.[36] Briefly, kinase activities of VEGFR1, PDGFRα, Tie-2, epidermal growth factor receptor (EGFR), insulin receptor (IR), insulin-like growth factor 1 receptor (IGF1-R), c-kit, Src and focal adhesion kinase (FAK) were determined by use of the AlphaScreen® system. For VEGFR1, kinase assay was performed with 20 ng/mL VEGFR1 (Millipore) and 0.5 μM ATP. For EGFR, kinase assay was performed with 50 ng/mL EGFR and 2 μM ATP. For IGF1-R, kinase assay was performed with 10 ng/mL IGF1-R (BIOMOL, USA) and 10 μM ATP. For FAK, kinase assay was performed with 62 ng/mL FAK (N-terminal FLAG-tagged recombinant proteins using the baculovirus expression system) and 2 μM of ATP. In these assays, wells containing the substrate and the enzyme without the compound were used as total reaction control. Wells containing the biotinylated poly-GluTyr (4:1) and the enzyme without ATP were used as basal control. B-raf, extracellular signal-regulated kinases (ERK1), protein kinase Cθ (PKCθ), glycogen synthase kinase-3β (GSK-3β) and Aurora A kinase activity was determined by use of radio labeled [γ-^{33}P] ATP (GE Healthcare, USA). For GSK-3β, kinase assay was performed with 2 μg/mL GSK-3β, 4 μg/mL of pGS peptide and 0.5 μM ATP (0.1 μCi/50 μL/well of [γ-^{33}P] ATP). For Aurora A, kinase assay was performed with 10 μg/mL Aurora A, 30 μmol/L Aurora substrate peptide and 0.5 μM ATP (0.2 μCi/50 μL/well of [γ-^{33}P] ATP). HER2 kinase activity was determined by use of radio labeled [γ-^{32}P] ATP (GE Healthcare). In these assays, wells containing the substrate and the enzyme without the compound were used as total reaction control. Wells containing the substrate and the radio labeled ATP without the enzyme was used as basal control. The concentration of inhibitor producing 50% inhibition of the kinase activities (IC$_{50}$ values) and 95% confidence intervals (95% CI) were analyzed as described above.

5.50. Cell proliferation assay

HUVECs (Cambrex, USA) were seeded into a 96-well plate at 3000 cells/well in Human Endothelial-SFM Growth Medium (Invitrogen) containing 3% fetal bovine serum (FBS) (Hyclone, USA) and were incubated overnight at 37 °C in a 5% CO$_2$ incubator. Various concentrations of the test compounds were added in the presence of 60 ng/mL VEGF (R&D systems, USA), and the cells were cultured for a further 5 days. Cellular proliferation was determined by the WST-8 formazan assay using Cell Counting Kit-8 (DOJINDO Laboratories, Japan). Briefly, 10 μL/well of Cell Counting Kit-8 was added and the cells were cultured for several hours. Then, the absorbance value at 450 nm was measured using a Benchmark Plus Microplatereader (Bio-Rad Labs., USA). The IC$_{50}$ values and 95% confidence intervals (95% CI) were calculated from a dose–response curve generated by least-squares linear regression of the response using NLIN procedure of the SAS software (SAS Institute Japan, Inc., Japan).

5.51. Pharmacokinetic studies

Test compounds were administered at a dose of 10 mg/kg as a cassette dosing to nonfasted mice. After oral administration, blood samples were collected. The blood samples were centrifuged to obtain the plasma fraction. The plasma samples were deproteinized with acetonitrile containing an internal standard. After centrifugation, the supernatant was diluted with a mixture of 0.01 mol/L ammonium formate solution and acetonitrile (9:1, v/v) and centrifuged again. The compound concentrations in the supernatant were measured by LC/MS/MS.

5.52. Xenograft nude mouse model

Human prostate carcinoma cell line DU145 (ATCC No. HTB-81) was obtained from American Type Culture Collection (Manassas, USA). The cells were proliferated in RPMI1640 (Invitrogen Corp) supplemented with 10% heat-inactivated fetal bovine serum (Hy-Clone) and antibiotics (100 units/mL penicillin G and 100 μg/mL streptomycin, Wako Pure Chemical, Japan). The cells were cultured in tissue culture dishes in a humidified incubator at 37 °C in an atmosphere of 5% CO$_2$ and 95% air. The hydrochloride salt of **20d** was suspended in vehicle solution including 1% citric acid (Wako Pure Chemical) and 1% gum arabic (Suzu Pharmaceutical, Japan) solution.

Six-week old male athymic nude mice (BALB/cA Jcl-nu/nu, Japan Clea, Japan) received subcutaneous injections into the hind flank with 3×10^6 DU145 cells in 100 μL of 1:1 volume mixture of Hanks' balanced salt solution (GIBCO, Invitrogen Corp, USA) and Matrigel (BD Biosciences, CA, USA). When tumors reached a volume of 150–210 mm^3, mice were randomized into groups of 5 ($n = 5$). Then, mice were orally given vehicle or the hydrochloride salt of **20d** (1.5, 3, 6 and 12 mg/kg) twice-daily for 3 weeks.

Tumor volumes were assessed by bilateral vernier caliper measurement twice-weekly after inoculation and calculated as volume = length × width^2 × 1/2, where length was taken to be the longest diameter across the tumor and width the corresponding perpendicular. Treatment over control (T/C, %), an index of antitumor efficacy, was calculated by comparison of the mean change in tumor volume over the treatment period for the control and treated groups. Body weight was also measured on the day of tumor volume assessment. Effects of the hydrochloride salt of **20d** on tumor growth and body weight were statistically analyzed by a one-tailed Williams' test. Differences were considered significant at $p \leqslant 0.025$.

References and notes

1. Folkman, J. N. Eng. J. Med. **1971**, 285, 1182.
2. Weidner, N. Am. J. Pathol. **1995**, 147, 9.
3. Zetter, B. R. Annu. Rev. Med. **1998**, 49, 407.
4. Ferrara, N.; Kerbel, R. S. Nature **2005**, 438, 967.
5. Olsson, A. K.; Dimberg, A.; Kreuger, J.; Claesson-Welsh, L. Nat. Rev. Mol. Cell Biol. **2006**, 7, 359.
6. Rak, J.; Mitsuhashi, Y.; Bayko, L.; Filmus, J.; Shirasawa, S.; Sasazuki, T.; Kerbel, R. S. Cancer Res. **1995**, 55, 4575.
7. Zhang, L.; Yu, D.; Hu, M.; Xiong, S.; Lang, A.; Ellis, L. M.; Pollock, R. E. Cancer Res. **2000**, 60, 3655.
8. Mukhopadhyay, D.; Knebelmann, B.; Cohen, H. T.; Ananth, S.; Sukhatme, V. P. Mol. Cell. Biol. **1997**, 17, 5629.
9. Ferrara, N.; Gerber, H. P.; LeCouter J. Nat. Med. **2003**, 9, 669.
10. Forsythe, J. A.; Jiang, B.; Iyer, N. V.; Agani, F.; Leung, S. W.; Koos, R. D.; Semenza, G. L. Mol. Cell. Biol. **1996**, 16, 4604.
11. Shweiki, D.; Itlin, A.; Soffer, D.; Keshet, E. Nature **1992**, 359, 843.
12. Rahimi, N. Exp. Eye Res. **2006**, 83, 1005.

13. Guetz, G. D.; Uzzan, B.; Nicolas, P.; Cucherat, M.; Morere, J. F.; Benamouzig, R.; Breau, J. L.; Perret, G. Y. *Br. J. Cancer* **2006**, *94*, 1823.
14. Yuan, A.; Yu, C.; Chen, W.; Lin, F.; Kuo, S.; Luh, K.; Yang, P. *Int. J. Cancer* **2000**, *89*, 475.
15. Jacobsen, J.; Grankvist, K.; Rasmuson, T.; Bergh, A.; Landberg, G.; Ljungberg, B. *Br. J. Urol. Int.* **2004**, *93*, 297.
16. Hurwitz, H.; Fehrenbacher, L.; Novotny, W.; Cartwright, T.; Hainsworth, J.; Heim, W.; Berlin, J.; Baron, A.; Griffing, S.; Holmgren, E.; Ferrara, N.; Fyfe, G.; Rogers, B.; Ross, R.; Kabbinavar, F. *N. Eng. J. Med.* **2004**, *350*, 2355.
17. Sandler, A.; Gray, R.; Perry, M. C.; Brahmer, J.; Schiller, J. H.; Dowlati, A.; Lilenbaum, R.; Johnson, D. H. *N. Eng. J. Med.* **2006**, *355*, 2542.
18. Miller, K.; Wang, M.; Gralow, J.; Dickler, M.; Cobleigh, M.; Perez, E. A.; Shenkier, T.; Cella, D.; Davidson, N. E. *N. Eng. J. Med.* **2007**, *357*, 2666.
19. Traxler, P.; Furet, P. *Pharmacol. Ther.* **1999**, *82*, 195.
20. Liu, Y.; Gray, N. S. *Nat. Chem. Biol.* **2006**, *2*, 358.
21. Pargellis, C.; Tong, L.; Churchill, L.; Cirillo, P. F.; Gilmore, T.; Graham, A. G.; Grob, P. M.; Hickey, E. R.; Moss, N.; Pav, S.; Regan, J. *Nat. Struct. Biol.* **2002**, *9*, 268.
22. Fabian, M. A.; Biggs, W. H., III; Treiber, D. K.; Atteridge, C. E.; Azimioara, M. D.; Benedetti, M. G.; Carter, T. A.; Ciceri, P.; Edeen, P. T.; Floyd, M.; Ford, J. M.; Galvin, M.; Gerlach, J. L.; Grotzfeld, R. M.; Herrgard, S.; Insko, D. E.; Insko, M. A.; Lai, A. G.; Lélias, J.; Mehta, S. A.; Milanov, Z. V.; Velasco, A. M.; Wodicka, L. M.; Patel, H. K.; Zarrinkar, P. P.; Lockhart, D. J. *Nat. Biotech.* **2005**, *23*, 329.
23. Ishikawa, T.; Taniguchi, T.; Banno, H.; Seto, M. WO 2005118588; Chem. Abstr. 2006, 144, 36371.
24. Furneaux, R. H.; Tyler, P. C. *J. Org. Chem.* **1999**, *64*, 8411.
25. Evans, G. B.; Furneaux, R. H.; Hutchison, T. L.; Kezar, H. S.; Morris, P. E., Jr.; Schramm, V. L.; Tyler, P. C. *J. Org. Chem.* **2001**, *66*, 5723.
26. Ullman, E. F.; Kirakossian, H.; Singh, S.; Wu, Z. P.; Irvin, B. R.; Pease, J. S.; Switchenko, A. C.; Irvine, J. D.; Dafforn, A.; Skold, C. N.; Wagner, D. B. *Proc. Natl. Acad. Sci. U.S.A.* **1995**, *92*, 3566.
27. Copeland, R. A. *Methods Biochem. Anal.* **2005**, *46*, 1.
28. Wood, E. R.; Truesdale, A. T.; McDonald, O. B.; Yuan, D.; Hassell, A.; Dickerson, S. H.; Ellis, B.; Pennisi, C.; Horne, E.; Lackey, K.; Alligood, K. J.; Rusnak, D. W.; Gilmer, T. M.; Shewchuk, L. *Cancer Res.* **2004**, *64*, 6652.
29. Swinney, D. C. *Nat. Rev. Drug Disc.* **2004**, *3*, 801.
30. Liu, T.; Toriyabe, Y.; Kazak, M.; Berkman, C. E. *Biochemistry* **2008**, *47*, 12658.
31. Manning, G.; Whyte, D. B.; Martinez, R.; Hunter, T. *Science* **2002**, *298*, 1912.
32. Thurston, G. *Cell Tissue Res.* **2003**, *314*, 61.
33. Pietras, K.; Sjöblom, T.; Rubin, K.; Heldin, C. H.; Östman, A. *Cancer Cell* **2003**, *3*, 439.
34. Abramsson, A.; Lindblom, P.; Betsholtz, C. *J. Clin. Invest.* **2003**, *112*, 1142.
35. Connolly, J. M.; Rose, D. P. *J. Urol.* **1998**, *160*, 932.
36. Saitoh, M.; Kunitomo, J.; Kimura, E.; Hayase, Y.; Kobayashi, H.; Uchiyama, N.; Kawamoto, T.; Tanaka, T.; Mol, C. D.; Dougan, D. R.; Textor, G. S.; Snell, G. P.; Itoh, F. *Bioorg. Med. Chem.* **2009**, *17*, 2017.